HOW DOES BINOCULAR RIVALRY

EMERGE FROM CORTICAL MECHANISMS OF 3-D VISION?

Stephen Grossberg, Arash Yazdanbakhsh, Yongqiang Cao, and Guru Swaminathan[1]

Department of Cognitive and Neural Systems
and
Center for Adaptive Systems
Boston University
677 Beacon Street, Boston, MA 02215
Phone: 617-353-7858
Fax: 617-353-7755

Submitted: July, 2007

Technical Report CAS/CNS-2007-010

All correspondence should be addressed to

Professor Stephen Grossberg
Department of Cognitive and Neural Systems
Boston University
677 Beacon Street
Boston, MA 02215

Phone: 617-353-7858/7857

Fax: 617-353-7755

Email:steve@bu.edu

[1] SG was supported in part by the National Science Foundation (NSF SBE-0354378) and the office of Naval Research (ONR N00014-01-1-0624). AY was supported in part by the Air Force Office of Scientific Research (AFOSR F49620-01-1-0397) and the Office of Naval Research (ONR N00014-01-1-0624). YC was supported by the National Science Foundation (NSF SBE-0354378). GS was supported in part by the Air Force Office of Scientific Research (AFOSR F49620-98-1-0108 and F49620-01-1-0397), the National Science Foundation (NSF IIS-97-20333), the Office of Naval Research (ONR N00014-95-1-0657, N00014-95-1-0409, and N00014-01-1-0624), and the Whitaker Foundation (RG-99-0186).

Abstract

Under natural viewing conditions, a single depthful percept of the world is consciously seen. When dissimilar images are presented to corresponding regions of the two eyes, binocular rivalry may occur, during which the brain consciously perceives alternating percepts through time. How do the same brain mechanisms that generate a single depthful percept of the world also cause perceptual bistability, notably binocular rivalry? What properties of brain representations correspond to consciously seen percepts? A laminar cortical model of how cortical areas V1, V2, and V4 generate depthful percepts is developed to explain and quantitatively simulate binocular rivalry data. The model proposes how mechanisms of cortical development, perceptual grouping, and figure-ground perception lead to single and rivalrous percepts. Quantitative model simulations of perceptual grouping circuits demonstrate influences of contrast changes that are synchronized with switches in the dominant eye percept, gamma distribution of dominant phase durations, piecemeal percepts, and coexistence of eye-based and stimulus-based rivalry. The model as a whole also qualitatively explains data about the involvement of multiple brain regions in rivalry, the effects of object attention on switching between superimposed transparent surfaces, monocular rivalry, Marroquin patterns, the spread of suppression during binocular rivalry, binocular summation, fusion of dichoptically presented orthogonal gratings, general suppression during binocular rivalry, and pattern rivalry. These data explanations follow from model brain mechanisms that assure non-rivalrous conscious percepts.

Keywords: Visual cortex, binocular vision, binocular rivalry, perceptual grouping, orientational competition, synaptic habituation, surface perception, V1, V2, V4, consciousness, LAMINART model

Introduction

Neuroscience has progressed further in understanding how the brain sees than in many other areas of biological intelligence. Yet bridging the gap between individual neurons and conscious visual percepts remains a major challenge. The study of percepts like binocular rivalry and, more generally, bistable perception, has provided an informative probe of the dynamics of visual perception, even though such oscillating percepts are not the norm during natural vision. How do brain mechanisms that are used for normal three-dimensional (3-D) vision cause the oscillating properties of binocular rivalry? What actually rivals during binocular rivalry? This article provides a detailed answer to these questions that explains many data about rivalry while linking these explanations to mechanisms of non-rivalrous conscious 3-D vision.

Binocular rivalry is caused by presenting dissimilar images to corresponding regions of the two eyes. The two images compete for perceptual dominance, and one image can dominate conscious awareness for several seconds at a time, after which the previously suppressed image can be perceived. Rivalry has been described and analyzed for several hundred years (Blake and Logothetis 2002; Fox, 1991) during which psychophysical and neurobiological studies have identified a wide range of rivalry properties under different experimental conditions. Such data include: influences of contrast changes that are synchronized with switches in the dominant eye percept (Mueller and Blake, 1989); a gamma distribution of dominant phase durations (Levelt, 1967); piecemeal percepts whereby a mixture of rivalrous orientations (e.g., vertical and horizontal) that dominate at the same time in different locations evolves into an almost complete dominance by one of these orientations (Blake, O'Shea, and Mueller, 1992; Mueller and Blake, 1989; Ngo et al., 2000); percepts of both "stimulus rivalry" (Logothetis et al., 1996) and "eye rivalry" (Lee and Blake, 1999) under different experimental conditions of swapping orthogonal monocular gratings between the two eyes at different stimulus contrasts and swapping rates; effects of object attention on switching between superimposed transparent surfaces (Mitchell, Stoner, and Reynolds, 2004); correlations between rivalry percepts and neuron properties at higher levels of visual cortex (Logothetis and Schall, 1989; Sheinberg and Logothetis, 1997), as well as correlations with neuronal activity in human primary visual cortex, which is 55% as large as that evoked by alternately presenting the two monocular images without rivalry (Polonsky et al., 2000); and monocular rivalry, whereby a grid flashed to one eye breaks down into its individual oriented components that compete for visibility in a manner similar to what happens during binocular rivalry (Breese, 1899; Campbell and Howell, 1972; Sindermann and Lueddeke, 1972). The model proposed herein quantitatively simulates or qualitatively explains all these data, among others.

Models of binocular rivalry typically describe a circuit with two populations of cells that oscillate with respect to one another with temporal properties similar to rivalry oscillations (Arrington, 1993; Freeman 2005, Laing and Chow, 2002; Lankheet, 2006; Matsuoka, 1984; Mueller, 1990; Mueller and Blake, 1989; Stollenwerk and Bode 2003; Wilson 2003, 2005). See Table 1. These models typically are not designed to receive visual images and do not have an internal representation of a visual percept. A stronger test of a correct explanation of rivalry is to show how a model of normal 3-D vision, which explains and simulates visual percepts under normal viewing conditions, can also undergo binocular rivalry.

Among these models, two notable recent contributions are those of Wilson (2003) and Freeman (2005). Wilson (2003) suggested a two level competitive model. Level 1 is composed of two monocular cells representing the left and right eyes, which inhibit each other by inter-ocular inhibitory connections. The model was used to simulate the Flicker and Swap (F&S) "stimulus rivalry" paradigm of Logothetis et al (1996) during which 18 Hz on-off flicker of orthogonal monocular gratings, coupled with swapping the gratings between eyes at 1.5 Hz, does not change slow rivalry alternations. To explain these data, Wilson added a binocular level composed of two neurons that mutually inhibit each other. The F&S paradigm skips the first competitive level and let both left and right eye monocular cells remain active during swapping of the eyes' stimuli. Therefore, the only remaining source of rivalry is the binocular stage whose two neurons inhibit each other.

The Freeman (2005) multi-level model consists of four cells for each level, including two cells for each eye that have orthogonal preferred orientations. Left and right eye cells with the same preferred orientation have positive connection weights to the binocular cell at the next level with the same preferred orientation. Monocular cells with orthogonal preferred orientations have negative connection weights to the binocular cell at the next level. The Freeman (2005) model can simulate the increasing strength of the rivalry in higher cortical areas, as well as the gamma distribution and the lack of correlation between successive dominance durations.

Lee and Blake (1999) showed that the F&S stimulus rivalry effect in Logothetis et al. (1996) occurs only when contrast is low and swapping is fast. With high contrast and slow swapping, subjects reported rapid rivalry alternations, or "eye rivalry". Neither Wilson (2003, 2005) nor Freeman (2005) simulated the rapid eye rivalry alternation phenomenon of Lee and Blake (1999). Our model can simulate both the stimulus and eye rivalry effects under their respective stimulus conditions.

More importantly, neither the Freeman or Wilson model includes the process of perceptual grouping, which has long been known to play an important role in binocular rivalry. An excellent example of this fact is the experiment of Kovács, Papathomas, Yang, and Fehér (1996) in which they cut up images of a monkey's face and of a jungle scene into equal numbers of pieces, and exchanged half the pieces to form two composite images, with each image consisting of half the pieces corresponding to each of the original images. Each eye was presented with one of these composite images. If rivalry always occurred between the eyes, the observers should have reported seeing alternations between the two composite images. Instead, observers reported seeing alternations between the monkey's face and the jungle scene. This is just the sort of binocular reorganization that perceptual grouping can achieve.

Perceptual grouping is the process whereby spatially distributed visual features become linked into object boundary representations. Illusory contours are familiar examples of perceptual grouping, but grouping also binds together contiguous perceptual boundary fragments that individually receive bottom-up sensory inputs, as in the case of the composite images.

The claim that perceptual grouping is a key process in binocular rivalry helps to clarify why, despite the fact that binocular rivalry was discovered in 1760 by Dutour, it is still a topic of current research. If perceptual grouping is a key process in 3-D vision and figure-ground perception, then the task of understanding binocular rivalry is closely tied to the great challenge of characterizing the functional units of conscious 3-D perception.

Author	Levelt (1967) Data	Muller and Blake (1989) Data	Does both eye rivalry and stimulus rivalry	Explains patchy percepts	Explains rivalry from normal 3-D vision*	Explains rivalry-based V1 modulation	Uses visual input patterns
Matsuoka (1984)	No	No	No	No	No	No	No
Mueller (1990)	No	Yes	No	No	No	No	No
Laing and Chow (2002)	Yes	No slope simulation	No	No	No	No	No
Stollenwerk and Bode (2003)	Yes	Only CC paradigm	No	Yes	No	No	No
Wilson (2003)	Claims it would work if noise added	No	Yes	No	No	No	No
Freeman (2005)	Partially (Very long dominance durations)	Only CC paradigm	Yes	No	No	No	No
Lankheet (2006)	Yes	No	No	No	No	No	No
Grossberg et al (Our model)	Yes	Yes	Yes	Yes	Yes	Yes	Yes

*Explains how binocular rivalry emerges from cortical mechanisms of normal and fused 3-D vision.

Table 1. Properties of several biological rivalry models.

Methods and Results

Qualitative Explanation of Rivalry

As noted above, most existing models of binocular rivalry were not designed to receive visual images, do not have internal representations of visual percepts, and do not include a mechanism of perceptual grouping. Perceptual grouping is needed, however, to generate a coherent percept of any image or scene with a distributed spatial extent. Indeed, the FACADE model and its more recent laminar cortical version, the 3D LAMINART model, both predict that perceptual grouping, notably boundary completion, is a fundamental process in generating the perceptual representations that are consciously seen during normal 3-D vision. Here we further develop this theory to explain more data about binocular rivalry than alternative models.

The 3D LAMINART model has previously been developed to clarify how the laminar circuits of visual cortex achieve normal, unitary 3-D vision (e.g., Cao and Grossberg, 2005; Grossberg, 2003; Grossberg and Swaminathan, 2004; Grossberg and Yazdanbakhsh, 2005) and how these circuits develop from before birth into their adult form (Grossberg and Seitz, 2003). Here we show how model processes that contribute to normal 3-D visual development and perception can generate neural representations of rivalry percepts, and quantitatively simulate key data about binocular rivalry, when three

model processes that are used in perceptual grouping interact together in response to rivalry-inducing inputs. These results build on the qualitative explanation of binocular rivalry data that was given in Grossberg (1987), which was a precursor of the 3D LAMINART model, and which first modeled the primary role of perceptual grouping in explaining 3-D vision percepts. That article qualitatively explains a number of rivalry properties that are consistent with the current model, but that are not reviewed herein.

Our quantitative model simulations focus on perceptual grouping circuits to demonstrate their rate-limiting role in triggering binocular rivalry. Earlier articles have reviewed data supporting the prediction that these circuits occur in the pale stripes of cortical area V2. Qualitative explanations of rivalry data that involve many other brain regions are also summarized in terms of model mechanisms that represent processes from LGN through the boundary and surface processing streams through cortical areas V1, V2, and V4. We also use previously demonstrated properties of boundary and surface processes from LGN through cortical areas V1, V2, and V4 to qualitatively explain many other properties of rivalry data that follow directly from the quantitatively demonstrated grouping properties as they ramify through this larger system architecture. Previous studies of perceptual grouping during normal 3-D vision demonstrate how the same laws can generate stable non-rivalrous groupings in response to stimuli for which multiple possible groupings are not almost equally strong (e.g., Cao and Grossberg, 2005; Grossberg and Howe, 2003; Grossberg and Swaminathan, 2004; Grossberg and Yazdanbakhsh, 2005). Indeed, Grossberg and Swaminathan (2004) demonstrate this for groupings that are slanted in depth, and then go on to show that the same grouping laws can generate an oscillating 3-D percept of the Necker cube.

The three mechanisms of *perceptual grouping* that are needed to quantitatively simulate key data about binocular rivalry are: (1) the bipole property, (2) orientational competition, and (3) synaptic habituation or depression. The fact that models with just two oscillating cells cannot simulate perceptual grouping illustrates why they have not clarified how visual cortex normally sees.

Bipole property: Neurophysiological, anatomical, and perceptual data (Bosking et al., 1997; Field, Hayes, and Hess, 1993; Hirsch and Gilbert, 1991; Kapadia et al., 1995; Kellman and Shipley, 1991; McGuire et al., 1991; von der Heydt, Peterhans, and Baumgartner, 1984; Tucker and Katz, 2003) support the prediction (e.g., Grossberg, 1984; Grossberg and Mingolla, 1985) that perceptual grouping is carried out in cortical areas V2 (and V1) by long-range excitatory and shorter-range inhibitory interactions (Figure 1a) in layers 2/3 that enable groupings to form inwardly between pairs or greater numbers of approximately collinear and like-oriented cells (Figure 1b), but not outwardly from a single dot or edge (Figures 1c), the so-called *bipole grouping* property. Binocular rivalry percepts illustrate the contour coherence that is characteristic of bipole-mediated long-range grouping (e.g., Ngo et al., 2000). See Appendix equations (1) – (6) for a rigorous definition of the bipole property.

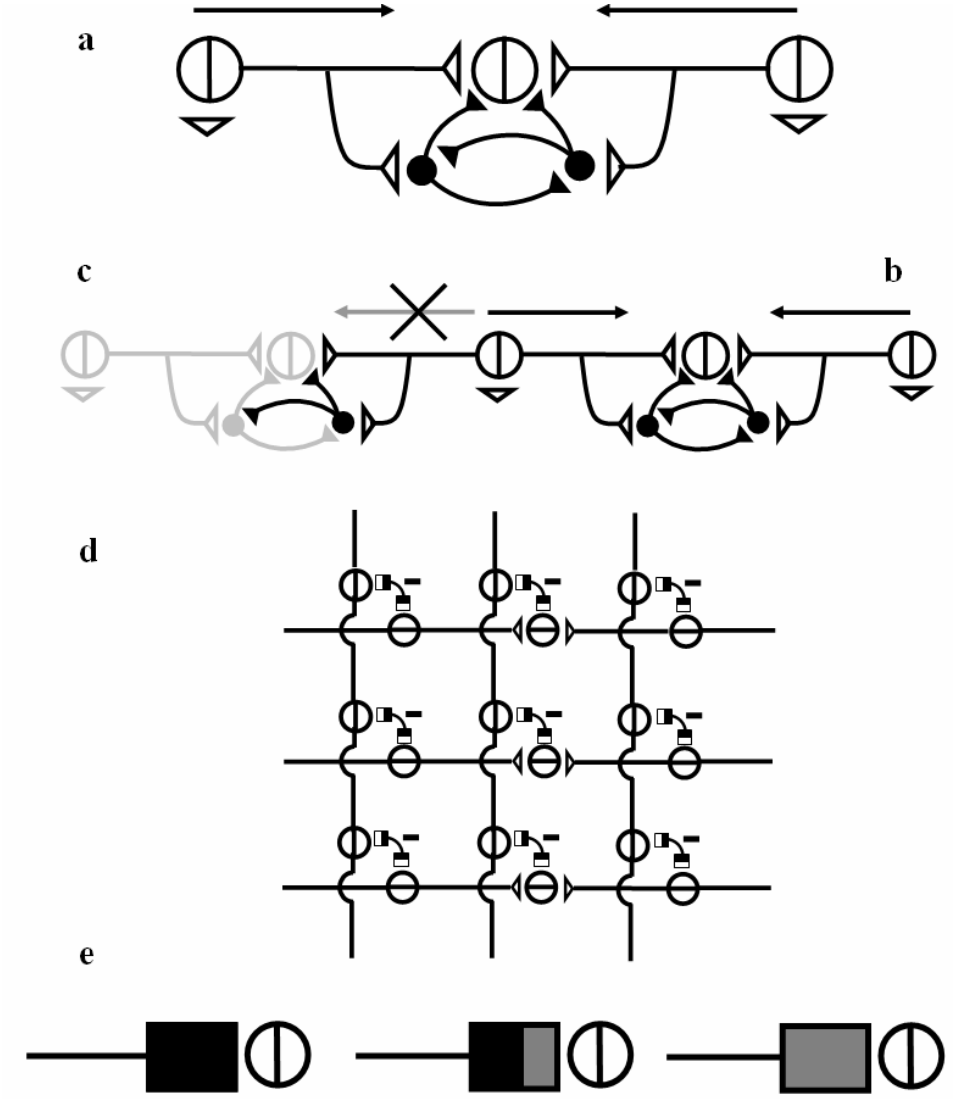

Figure 1. (a) bipole circuit; (b) bipole completes inwardly; (c) bipole does not complete outwardly; (d) orientational competition; (e) synaptic habituation. See text for details.

Orientational competition: Bipole cells that code nearby positions but different orientations compete to select a winning grouping at each position (Figure 1d). During 3-D figure-ground separation, orientational competition helps to determine percepts of occluding and occluded objects, both opaque and transparent (Grossberg and Swaminathan, 2004; Grossberg and Yazdanbakhsh, 2005; Kelly and Grossberg, 2000). It should also be noted that Grossberg (1987) proposed an explanation of how dichoptic rivalry displays produce a general suppression that is not feature specific; e.g., Blake and Fox (1974), Blake and Lema (1978), and Wales and Fox, 1970). Although our current discussion focuses on orientation-specific interactions, the 3D LAMINART model can also account for general suppression data. See Appendix equations (1) and (7) for a rigorous definition of orientational competition.

Synaptic habituation: Synaptic habituation (Francis et al., 1994; Grossberg, 1968, 1980), also called synaptic depression (Abbott et al., 1997), causes neuronal signals to become weaker through time in an activity-dependent manner (Figure 1e). That is, chemical transmitters that multiply, or gate, signals in active axons are inactivated, habituated, or depressed through time in an activity-dependent way. This mechanism plays an important role in several visual processes, including cortical development (Dragoi et al., 2001; Grossberg, 1980; Grunewald and Grossberg, 1998; Grossberg and Seitz, 2003), where it facilitates cortical map formation by preventing perseverative activation of initially favored cell populations, thereby enabling all the cells in the map to encode different combinations of features within a visual scene. In the adult, these same habituative mechanisms enable reset of adult perceptual representations in a form- and speed-sensitive manner as visual inputs change, thereby enabling unbiased processing of new visual inputs. This process also helps to explain data about visual persistence (Francis et al., 1994), aftereffects (Dragoi et al., 2001; Francis and Grossberg, 1996; Sur et al., 2002), adaptation (Abbott et al., 1997; Carpenter and Grossberg, 1981), motion perception (Ögmen and Gagné, 1990), visual category learning and hypothesis testing (Carpenter and Grossberg, 1990), and mental disorders (Grossberg and Seidman, 2006). See Appendix equations (1) and (7) – (9) for a rigorous definition of orientational competition.

These three perceptual grouping mechanisms work together as follows: When the visual system is presented with approximately balanced but conflicting inputs, as during binocular rivalry, a winning boundary is selected through cooperative bipole grouping and orientational competition. When the conflicting inputs have different orientations, orientational competition begins the process of inhibiting the more weakly activated orientation. If two or more V2 boundary cells, or cell populations, are activated that are collinear in space and favor the same orientation, the bipole property helps them to complete the boundary between them, thereby activating other cells between them that are tuned to the same orientation. Recurrent cooperative and competitive interactions among the bipole grouping and orientational competition cells help to fully suppress, and maintain suppression of, the activity of cells coding the losing orientation. At the same time, the boundary completion property of bipole grouping explains how partial dominance of units with the same orientation tuning can lead to a total dominance of that orientation (Ngo et al., 2000).

Given that positive feedback helps to select and maintain the activity of grouping cells that code the winning orientation, why does not the winning orientation persist forever due to hysteresis? In particular, when the vertically oriented signals are dominant, the bipole property insures the self-enhancement of vertical orientation signals, and orientational competition might never let the other orientation takes over. The third property of the model, synaptic habituation or depression, overcomes this problem: The chosen grouping weakens its active pathways through transmitter habituation in an activity-dependent way. The habituative transmitters are incorporated within recurrent, or feedback, interactions between the bipole cells that form the oriented boundary groupings (see Figures 1d and 1e). That enables the winning pathways to become selectively habituated, while the losing pathways can accumulate their transmitters. As this process continues cyclically through time, it leads to a rivalrous percept.

In summary, rivalry percepts arise from the laws for perceptual grouping. Figure 2a embeds these mechanisms within a larger laminar cortical model of how the brain forms perceptual groupings during normal 3-D vision. The three grouping mechanisms that are sufficient to drive parametric properties of rivalry occur within layer 2/3 of model area V2. These mechanisms have also been used to explain other phenomena about perceptual bistability, notably bistable 3-D percepts of a Necker cube (Grossberg and Swaminathan, 2004). Although these mechanisms are sufficient to explain how rivalry is initiated and maintained through time by perceptual grouping mechanisms, they cannot by themselves explain the percepts that are consciously seen during rivalry, just as they were not sufficient to explain conscious percepts of a Necker cube. This observation helps to clarify why neuronal activations in several different brain areas correlate with rivalry percepts.

If inputs in both eyes are parallel and fusable, rather than perpendicular or with other significantly non-colinear orientations, then they do not rival, because only the usual perceptual grouping properties are engaged, without activation of the cross-orientational competition that drives rivalry. Thus, the same model mechanism can support both non-rivalrous and rivalrous grouping. See the simulation in Figure 7 and Appendix A for further discussion.

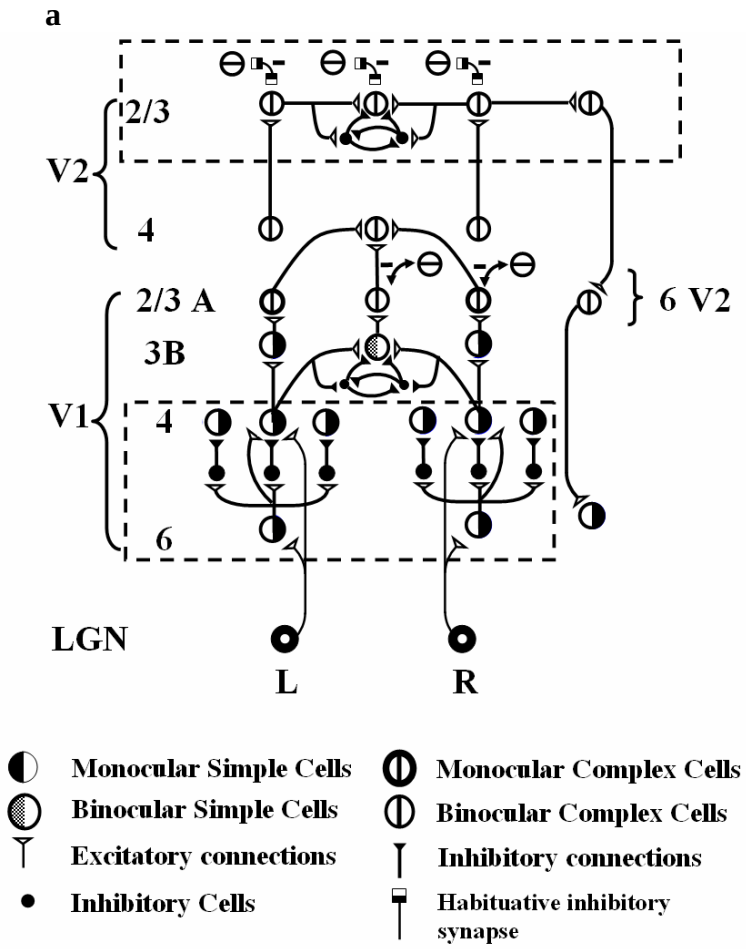

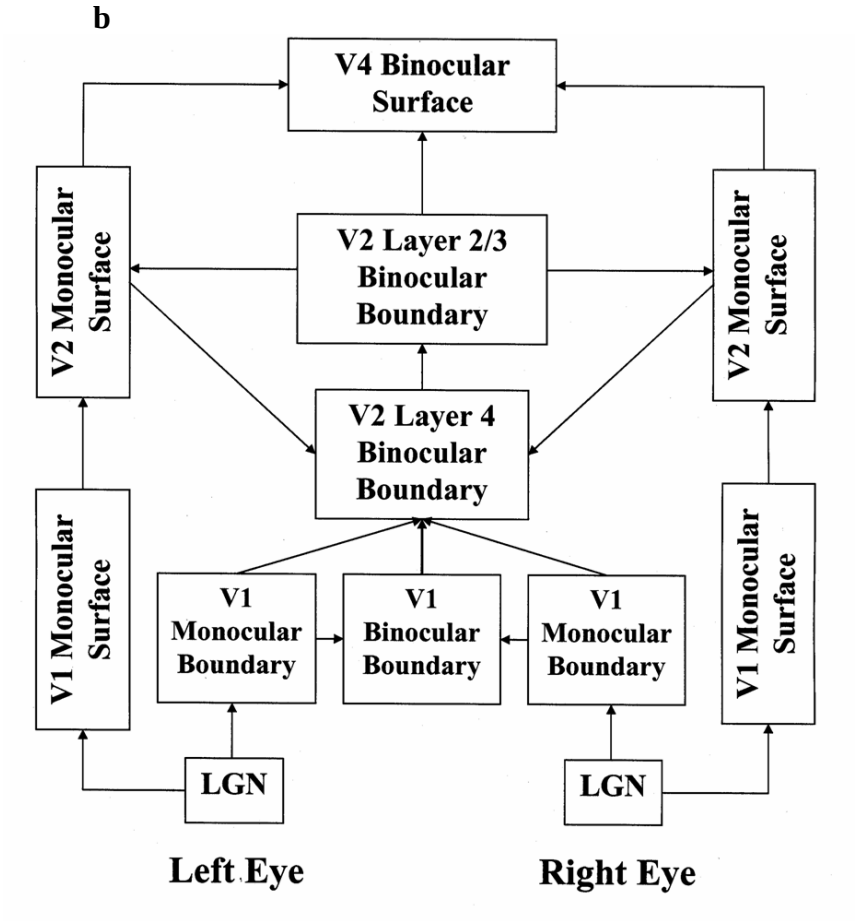

Figure 2. (a) Laminar circuits for boundary processing in cortical areas V1 and V2 within the 3D LAMINART model. V2 layer 2/3 of the model includes the three mechanisms that drive oscillations in response to binocular rivalry stimuli: bipole grouping, orientational competition, and synaptic habituation. Bipole grouping is realized by combining long-range excitatory interactions with self-normalizing di-synaptic inhibitory interactions. The other processing stages also play a role in explaining various rivalry data. (b) FACADE model macrocircuit of interactions between monocular and binocular boundary and surface representations. The model circuits in (a) and (b) were originally derived to explain data about non-rivalrous 3-D vision. Both boundary and surface representations are need to generate and to consciously see binocular rivalry percepts. See text for details.

Rivalry Influences Multiple Brain Regions: Amodal Boundaries and Visible Surfaces

Why cannot the perceptual groupings that drive rivalry oscillations completely explain rivalry percepts? This is so because perceptual groupings, or *boundaries*, are predicted to be amodal, or invisible, within the visual cortical processing stream within which they form, from LGN-to-(V1 interblobs)-to-(V2 pale stripes)-to-V4. Thus visible properties of rivalry percepts are not formed within the boundary stream that controls rivalry oscillations. A parallel cortical processing stream interacts with the boundary stream to

generate visible percepts of *surfaces*. Visible rivalry percepts are hereby predicted to be consciously seen in the surface perception stream from LGN-to-(V1 blobs)-to-(V2 thin stripes)-to-V4. Figure 2b shows a block diagram of 3D LAMINART processing stages that includes both boundary and surface processes. Many psychophysical studies have supported the prediction in Grossberg (1987) that 3-D boundaries and surfaces are the perceptual units of 3-D vision during non-rivalrous 3-D vision. Grossberg (2003) reviews psychophysical, neurophysiological, and anatomical data that support the predicted properties of these processes. The current model shows how these processes can also explain data about rivalrous vision. In particular, for both non-rivalrous and rivalrous vision, the following properties are needed to understand why both amodal boundaries and visible surfaces need to be computed.

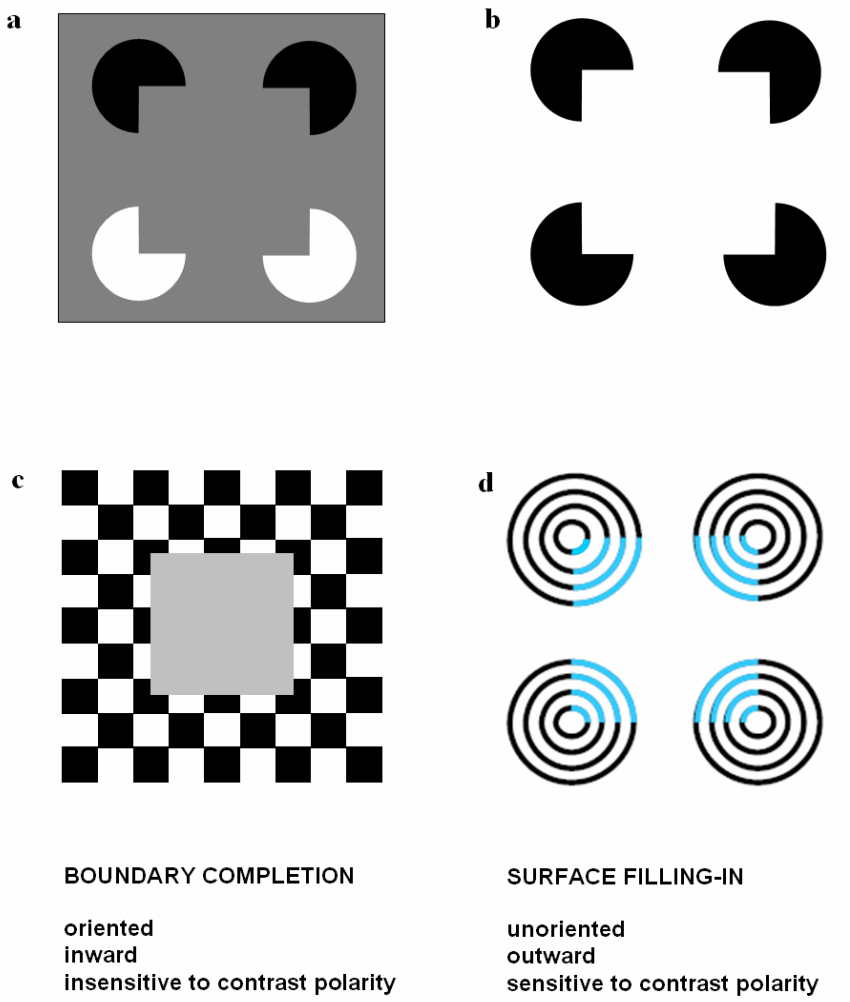

Figure 3. (a) Opposite-contrast Kanizsa square shows that both opposite-contrast polarity and same-contrast polarity collinear edges can group together, and that both sorts of groupings are part of the same boundary completion process. Because two pac men are darker than the background gray, and the other two are lighter than the background gray, they induce lightening and darkening effects that cancel out within the Kanizsa square, thereby creating an invisible, or

amodal, square percept that is recognized but not seen. (b) Same-contrast Kanizsa square is visible because all four black pac men induce brightness signals within the square that create a brighter square after surface filling-in. (c) Pooling of opposite contrast at every position along the border of the gray square illustrates how the brain can build an object boundary around a textured background and thus why "all boundaries are invisible." (d) Neon color spreading vividly illustrates the computationally complementary properties of boundary completion and surface filling-in that are summarized at the bottom of the figure.

Complementary rules for boundary and surface formation. Boundaries and surfaces are formed using *complementary* computational rules. Their streams interact to overcome their complementary deficiencies. Figures 3a and 3b illustrate these complementary properties using illusory contour percepts of Kanizsa squares. In these percepts, boundaries are recognized that form *inwardly* between cooperating pairs of incomplete disk (pac man) inducers to form the square's sides. These boundaries are *oriented* collinearly between like-oriented inducers.

The square boundary in Figure 3b can be both seen and recognized because of the enhanced illusory brightness of the Kanizsa square. The square boundary in Figure 3a can be recognized even though it cannot be seen; that is, there is no brightness or color difference on either side of the boundary. Figure 3a shows that *some* boundaries can be recognized even though they are invisible. LAMINART predicts that *all* boundaries are amodal, or invisible, within the boundary stream.

The boundary in Figure 3a is invisible, or amodal, because its vertical boundaries form between black and white inducers that possess opposite contrast polarity on the gray background. The same is true of the boundary around the gray square in Figure 3c. Figure 3c illustrates how, by pooling signals from opposite contrast polarities at each position, the brain can build a boundary around the entire square, even when it lies in front of a textured background whose contrasts reverse as the square's bounding edge is traversed. Pooling of opposite polarities to form the square boundary renders the boundary system output *insensitive* to contrast polarity. The boundary system cannot represent visible colors or brightnesses, because its output cannot signal the difference between dark/light vs. light/dark. The first stage in this pooling process is predicted to occur at complex cells in cortical area V1. Complex cells pool inputs from all achromatic and chromatic cell types that input to the cortex (Thorell et al., 1981) in order to use all available input contrasts to determine the location of scenic boundaries (Grossberg, 1987; Grossberg and Mingolla, 1985). In summary, "all boundaries are invisible" to enable the visual cortex to build boundaries around objects as a key step in object recognition.

If boundaries are invisible, then how do we see anything? The 3D LAMINART model, and its BCS/FCS and FACADE model precursors (Grossberg, 1984, 1994; Grossberg and Mingolla, 1985), predicts that visible properties of a scene are represented by the surface processing stream. A key step in representing a visible surface is called *filling-in*. Why does a surface filling-in process occur? An early stage of surface processing compensates for variable illumination, or "discounts the illuminant," in order to prevent fluctuating illuminant variations from distorting all percepts. Discounting the illuminant attenuates color and brightness signals except near regions of sufficiently rapid surface change, such as edges or texture gradients, which are relatively uncontaminated

by illuminant variations. Later stages of surface formation fill in the attenuated regions with these relatively uncontaminated color and brightness signals, and do so at the correct relative depths from the observer through a process called *surface capture*.

Figure 3d shows an example of surface filling-in that is called neon color spreading (Grossberg and Mingolla, 1985; Van Tuijl, 1975). Filling-in spreads *outwardly* from the individual blue inducers in all directions. Its spread is thus *unoriented*. The 3D LAMINART model predicts that signals from the boundary stream to the surface stream define the regions within which filling-in is restricted. Without these boundary signals, filling-in would dissipate across space, and no visible surface percept could form. Invisible boundaries hereby indirectly assure their own visibility through their interactions with the surface stream. Filling-in can lead to visible percepts because it is *sensitive* to contrast polarity. These complementary properties of boundary completion and surface filling-in are summarized at the bottom of Figure 3.

Amodal boundaries capture and contain visible surface properties. During binocular rivalry, the dominant boundaries support conscious visibility only of those surfaces that are consistent with them. Grossberg (1987, 1994) predicted cortical mechanisms whereby such boundary-selective surface capture can generate 3-D percepts. Grossberg and Swaminathan (2004), Grossberg and Yazdanbakhsh (2005), and Kelly and Grossberg (2000) simulated several kinds of 3-D percepts that depend upon such depth-selective boundary-mediated surface capture, notably figure-ground, transparency, and 3D neon percepts. How surface capture leads to visible 3-D percepts is one of the main reasons why multiple levels of visual cortex participate in generating conscious percepts of binocular rivalry: Although key steps in rivalry induction may occur in the boundary processes within V2 pale stripes, they can propagate to the surface processes in V2 thin stripes that initiate figure-ground separation, to later boundary and surface processes in V4 that are predicted to generate consciously visible 3-D percepts, and to cortical areas beyond V4 where such percepts are recognized.

Attention, synchrony, learning, and consciousness. Feedback between these bottom-up processes and reciprocal top-down processes generates synchronous resonant states that focus attention, stabilize learning, and lead to consciously seen 3-D percepts. Such a linkage between attention, learning, and consciousness was predicted by Grossberg (1976, 1978, 1980) as part of his development of Adaptive Resonance Theory, or ART, and has received extensive behavioral and neurobiological experimental support. See reviews of relevant data in Engel, Fries, and Singer (2001), Fries, Reynolds, Rorie, and Desimone (2001), and Pollen (1999). Reviews of how ART provides a unified explanation of these data are provided in Gove, Grossberg, and Mingolla (1995), Grossberg (1995, 1999, 2003), and Raizada and Grossberg (2003). These top-down attentive processes include feedback from areas like V2 to earlier cortical areas like V1, as simulated in Gove, Grossberg, and Mingolla (1995), a fact that is important towards understanding how V1 cell properties reflect rivalry-inducing oscillations in the pale stripes of V2.

Experiments have reported data that show how multiple brain areas may oscillate with rivalry percepts. For example, using fMRI techniques, Polonsky et al. (2000) and Lee and Blake (2002) showed that modulated activity of V1 is related to the perceptual switch. Such data are consistent with the models of Blake (1989), Mueller (1990), and Lumer (1998), which assume that monocular competition causes rivalry, and therefore

that the generative rivalry circuit may be in V1. However, by recording from single neurons in V1, V2, and V4, while using an orthogonal grating stimulus, Leopold and Logothetis (1996) found many cells, particularly in V4, that have activity modulations related to the perceptual switch. Logothetis (1998) reported that such cells are almost exclusively binocular and their proportion increases in the higher processing stages of the visual system.

The early data of Diaz-Caneja (1928) also showed that rivalry may not just follow competition between the two eye views. Rather, it can also follow cross-ocular groupings that are induced between the two eyes, and thereby implicate perceptual grouping in the rivalry process. This observation does not reject monocular channel competition, but it does implicate higher-level competition as well. Polonsky et al. (2000) used different contrasts as ocularity tags, and found that fMRI responses of later visual areas, such as V2, V3, V3A, and V4, fluctuate strongly between higher and lower contrasts, but that V1 activity also fluctuates between higher and lower contrasts.

None of the data about stronger correlations with rivalry at higher cortical areas is inconsistent with V1 having BOLD modulated activity corresponding to the perceptual switch (Lee and Blake, 2002). As Figure 2a illustrates, top-down signals from the grouping dynamics in V2 to V1 can explain this result in the same way that they have explained how V2 groupings influence other V1 receptive field properties (Grossberg, 2003; Grossberg and Swaminathan, 2004).

The 3D LAMINART model clarifies these results by showing how the three grouping mechanisms of bipole grouping, orientational competition, and synaptic habituation can interact together to generate emergent properties that quantitatively simulate the temporal dynamics of several key rivalry experiments, while the total model system in Figure 2 clarifies how multiple areas work together to generate the consciously visible percepts that are seen during binocular rivalry.

Quantitative Data Simulations

Contrast-Duration Properties. The grouping dynamics of layer 2/3 of V2 in the model quantitatively simulate the data of Mueller and Blake (1989); see Table 2. In these experiments, the stimuli to the two eyes are orthogonal sinusoidal gratings. While the suppression and dominance phase duration is registered, the contrast of the test eye is manipulated in three different ways, corresponding to three paradigms: Continuous Contrast (CC), Synchronized Dominance (SD), and Synchronized Suppression (SS)

Contrast change Paradigm	Phase	Duration/Contrast Slope (Simulation)	Duration/Contrast Slope (Psychophysics)
SD	Dominant	0.92	0.86
	Suppression	0.24	0.20
SS	Dominant	– 0.03	– 0.06
	Suppression	– 0.70	– 0.73
CC	Dominant	0.30	0.28
	Suppression	– 0.74	– 0.77

Table 2. Data and model simulations of Mueller and Blake (1989).

In the CC paradigm, an increase or decrease in image contrast is independent of the suppression or dominance phase and contrast is constant during the suppression and dominance phase. In the SD paradigm, the increased contrast is synchronized with the dominance phase of the test eye, and in the SS paradigm with the suppression phase. Table 2 shows the slopes of linear regression fits to the duration-contrast data in the CC, SD, and SS paradigms. Because the model V2 layer 2/3 is binocular, the ocularity tag for the each stimulus is orientation. Therefore, changing the contrast of the test eye stimulus is accomplished by changing the contrast of one of the orientations (test orientation) and leaving the orthogonal orientation contrast constant.

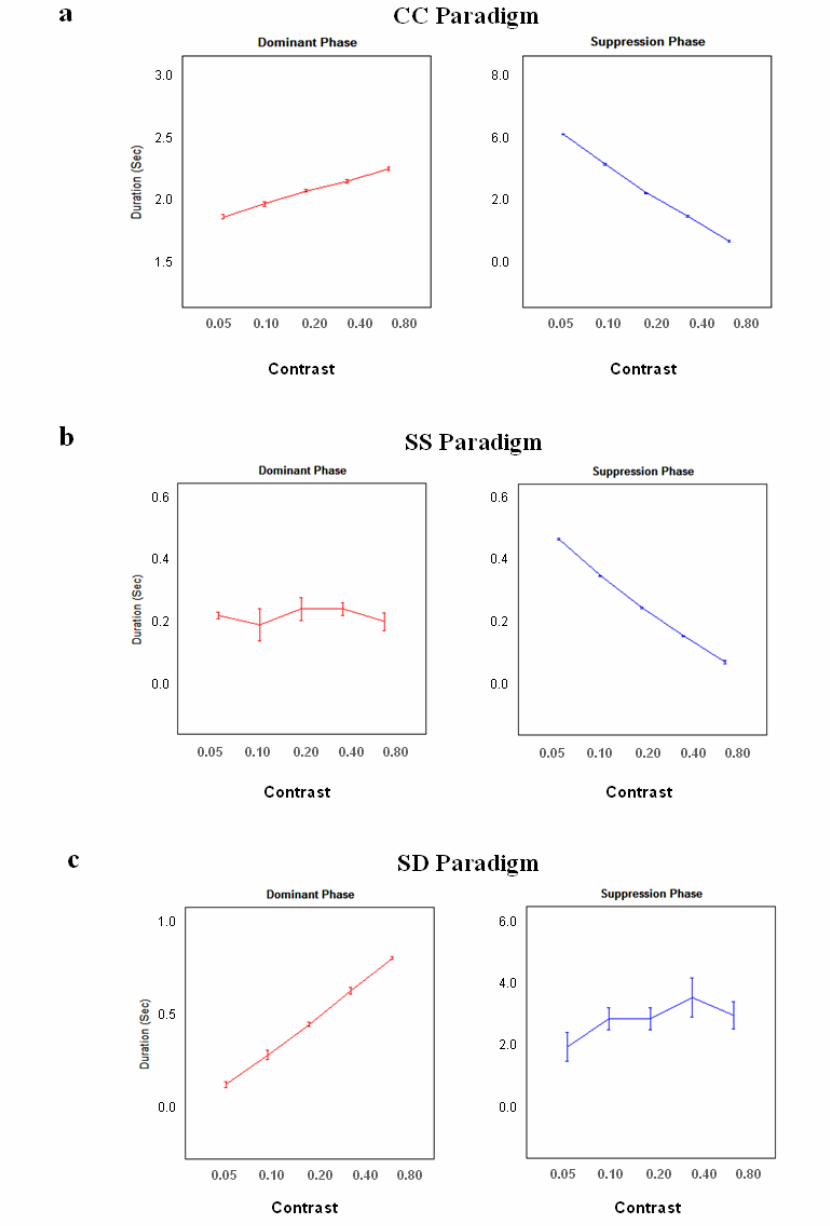

Figure 4. (a) Simulated time dynamics of CC paradigm: The simulation slope of the duration versus contrast is the same as that in the Mueller and Blake (1989)

results; see Table 2. The error bars shows the variability of duration at each contrast, which is consistent with their psychophysical experiment. The source of this variability in the simulation is a very small uniform random quantity in the habituative transmitter processes, which is a minimal biologically plausible assumption. (b) Simulation result for the SS paradigm. The linear regression slopes have the same sign and amplitude as that of Mueller and Blake (1989); see Table 2. (c) Simulation result for the SD paradigm. In general, the bottom-up input to layer 2/3 of V2 could be a nonlinear function of the contrast which impinges on the retina. In our simulations, we did not process the input prior to V2 apart from linearly expanding and shifting the input range. The input has the range of 0.05 to 0.80, as can be seen in the x axes. The linear transformation of the external input yielded an input to V2 within the range of 15.5 to 17.5. In particular, the input to V2 is derived from the abscissa values x in Figure 4 from the linear function $f(x) = 2.67x + 15/37$.

Figures 4a, 4b, and 4c, respectively, show the dominance and suppression durations, versus test orientation contrast, that resulted from stimulating the model V2 layer 2/3 with CC, SS, and SD stimuli. The x-axis of each curve plots the contrast of the test orientation to all V2 layer 2/3 model cells, and the y-axis shows the duration of dominance or suppression that is caused. Error bars reflect the standard deviation of dominance or suppression durations at each contrast. The simulations, like the data, show variability in durations at each contrast. Linear regression slopes were compared with the slopes in the data. By dividing the slope value of CC Dominant phase in the data over the simulation value, we calculated a scaling factor to compare simulation and data slopes. This scaling factor was multiplied by all simulation slope values. The data and scaled simulation values are shown in Table 2. Simulations fit the data well. Due to the nonlinear nature of the data, however, the values best convey the sign and ordinal relations, rather than exact numerical values. Mueller and Blake (1989) also emphasized data variability.

In the CC paradigm, when test orientation contrast increases, the inputs to corresponding V2 bipole cells increase too. As a result, the dominance duration of the test orientation increases with contrast while its suppression duration decreases, as shown in Figure 4a. In the SS paradigm, the change of test orientation contrast is synchronized with the suppression phase, and the contrast returns to a fixed constant level for all dominance phases. Therefore, the suppression duration decreases with contrast but the dominance duration has little changed, as shown in Figure 4b. The SD paradigm can be similarly explained. In summary, the main effects of contrast change in all the CC, SS, and SD paradigms can be explained as emergent properties of the perceptual grouping mechanisms of bipole grouping, orientational competition, and synaptic habituation acting together.

The variability of durations for each test contrast, which is quantitatively reflected in the error bars of both data and simulations, was experimentally described by Levelt (1967).

Gamma Distribution of Dominant Phase Durations. Levelt (1967) showed that the durations of the dominant phase, with constant contrasts, obey a gamma distribution. The variability in Figure 4 at each contrast arose from introducing neuronal noise into the

system: a small random value, taken uniformly from the interval (-0.15, 0.35), was added to the right side of the habituation equation during each integration step (see Appendix equations (8) and (9) below). Intuitively, the sum of such small independent random values typically obeys a normal distribution. Because the duration cannot be less than zero, a Gamma distribution obtains instead. The bipole cooperative synapses and orientational competition synapses have independent equations and thus habituate independently. This random process, which could be implemented in other ways as well, was used to simulate both the contrast-duration fits in Table 2 and the gamma distribution for dominance phase in Figure 5. To compute Figure 5, each duration was added to its corresponding bin in the histogram.

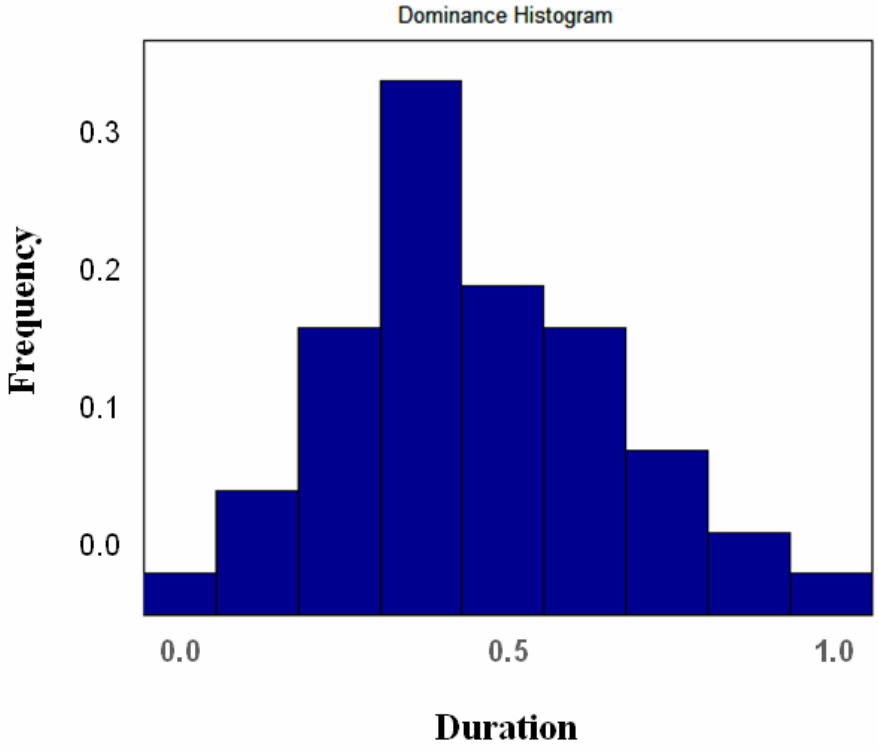

Figure 5. Simulation result for the duration distribution at one contrast. As Levelt (1967) noted, the dominant phase distribution is similar to gamma distribution, as was also found in the simulation.

The registered contrast in the x-axis of the above graph can be shifted to the left or right based on the selected contrast of the test stimulus. However, the gamma distribution pattern remains the same.

Mixed Phase Coherence. Binocular rivalry is not always a complete left eye, right eye, or coherent across-eye percept. Mixed phase percepts also occur (Blake, O'Shea, and Mueller, 1992; Mueller and Blake, 1989; Ngo et al., 2000). In general, emergent groupings are defined by contextual constraints across an entire scene or display. When these constraints interact with random fluctuations in such factors as receptive fields, internal noise, and attention, they can initially favor some orientations over others. The grouping property will attempt to complete inwardly whenever it has enough approximately coaxial and collinear activation on both sides of a region.

Collinear groupings due to bipole cooperation range from a length less than the bipole excitatory kernel size to a full field grouping when bipoles recurrently cooperate across space. Figure 6 shows a sequence of rivalrous groupings through time in which a vertical patchy percept becomes a global vertical grouping before a horizontal patchy grouping becomes a global horizontal grouping. All three grouping properties play a role in generating such rivalrous sequences. This grouping mechanism is consistent with data showing interocular grouping in rivalry Diaz-Caneja, 1928; Kovács, Papthomas, Yang, and Feher, 1996; Wade, 1973), since grouping cells within model layer 2/3 of V2 receive inputs from both eyes (Figure 2a). This model property is also consistent with neurophysiological data showing that V2 is mainly binocular (Hubel and Livingstone, 1987; Roe and Ts'o, 1997), disparity-sensitive (Peterhans, 1997; Poggio and Fischer, 1977; von der Heydt, Zhou, and Friedman, 2000), and is capable of long-range perceptual grouping (Peterhans and von der Heydt, 1989; von der Heydt, Peterhans, and Baumgartner, 1984).

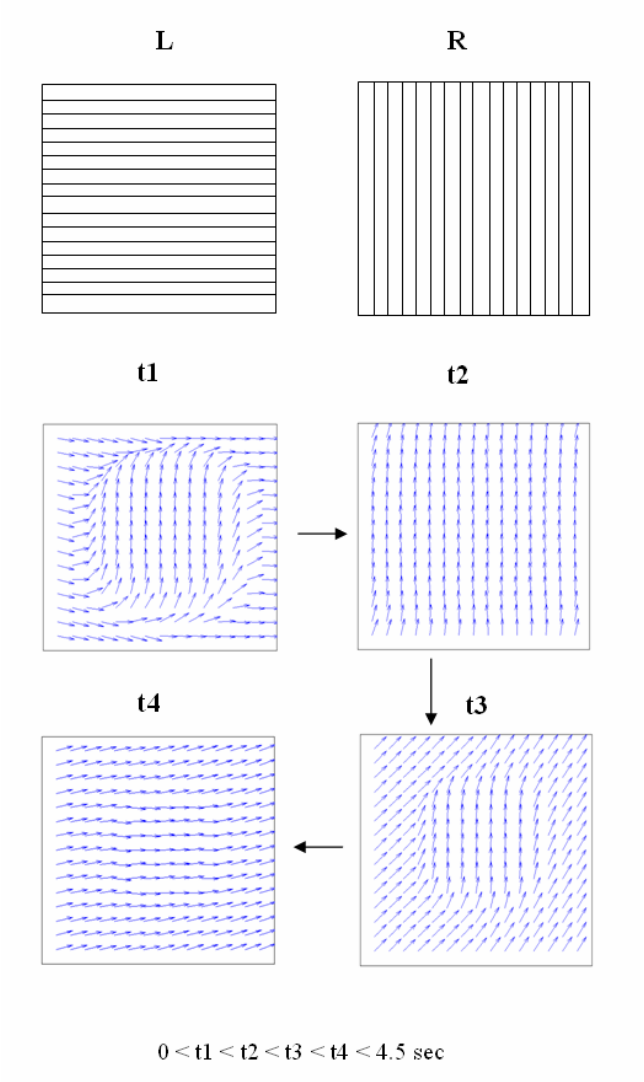

Figure 6. An illustration of how patchy groupings become global during a binocular rivalry sequence in response to mutually orthogonal gratings: (a) a

patchy grouping with horizontal and vertical orientations resolves in (b) into a vertical global grouping. (c) The perpendicular orientation starts to get instated in a patchy percept which resolves in (d) into a horizontal global grouping. The small needles are the vector sum of horizontal and vertical units. Oblique lines denote the transient mixture of horizontal and vertical orientations as the switch occurs between pure horizontals and verticals. There is no fixed duration for each phase. Their time dynamics and distribution are shown in Figures 4 and 5, which are consistent with the Mueller and Blake (1989) data. . What is actually seen by a human observer will depend on how long each grouping lasts, since it takes time for the surface representations to generate visible percepts in response to their inducing boundary groupings.

Figure 7 shows that, when only horizontally oriented inputs are presented to both eyes, so that there are no vertical inputs to compete with them, then the network converges to an equilibrium state with persistent horizontal groupings. Thus both a stable percept and a rivalrous percept can be generated by the same grouping network, with the same model parameters, under different stimulus conditions.

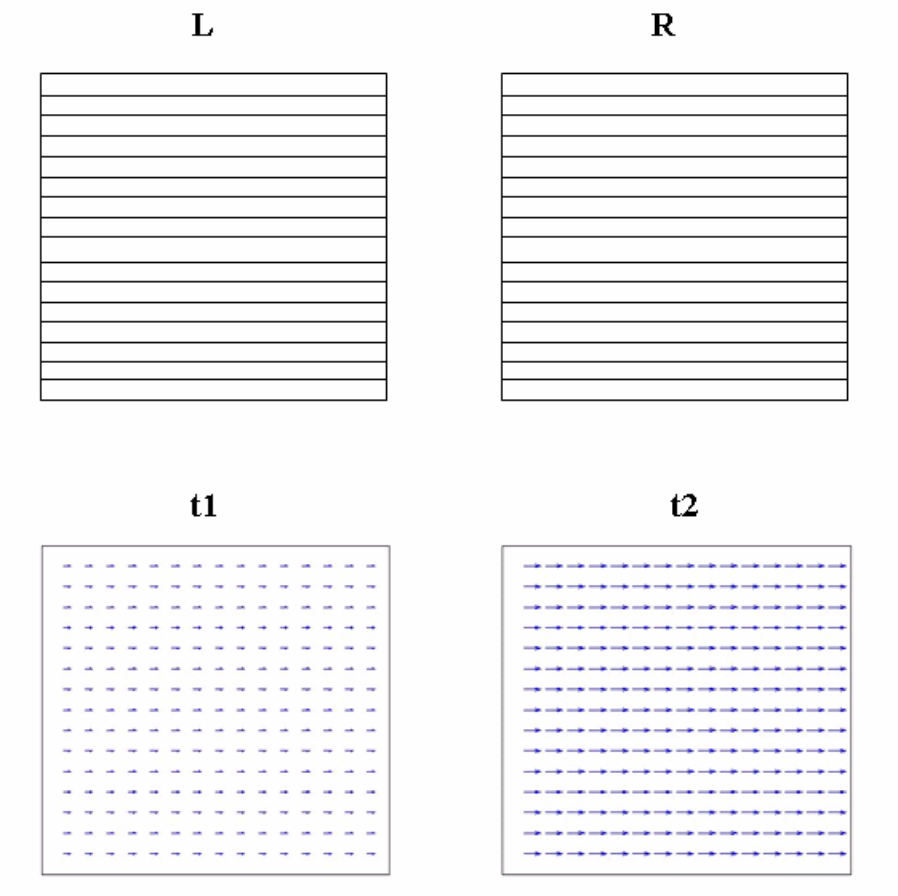

Figure 7. In the non-rivalrous case where both the left and right eye inputs are horizontal lines, the network gradually converges to a stable equilibrium (see time $t = t_2$), in which only horizontal orientations are active. Time $t = t_1 < t_2$ shows an intermediate state during the convergence process.

Coexistence of Stimulus Rivalry and Eye Rivalry. This section summarizes model simulations of the Flicker and Swap *stimulus rivalry* data of Logothetis et al (1996), as well as the *eye rivalry* data of Lee and Blake (1999). Logothetis et al (1996) showed that 18 Hz on-off flicker of orthogonal monocular gratings, coupled with swapping between the eyes at 1.5 Hz (333 ms per swap), does not change the smooth and slow rivalry alternations with dominance durations of about 2.35 seconds, which span approximately 7 swaps. These data challenge the monocular channel hypothesis. Lee and Blake (1999) found that this result holds only when stimulus contrast is low and swapping is slow. Otherwise, eye rivalry dominates during which rapid rivalry alternations occur.

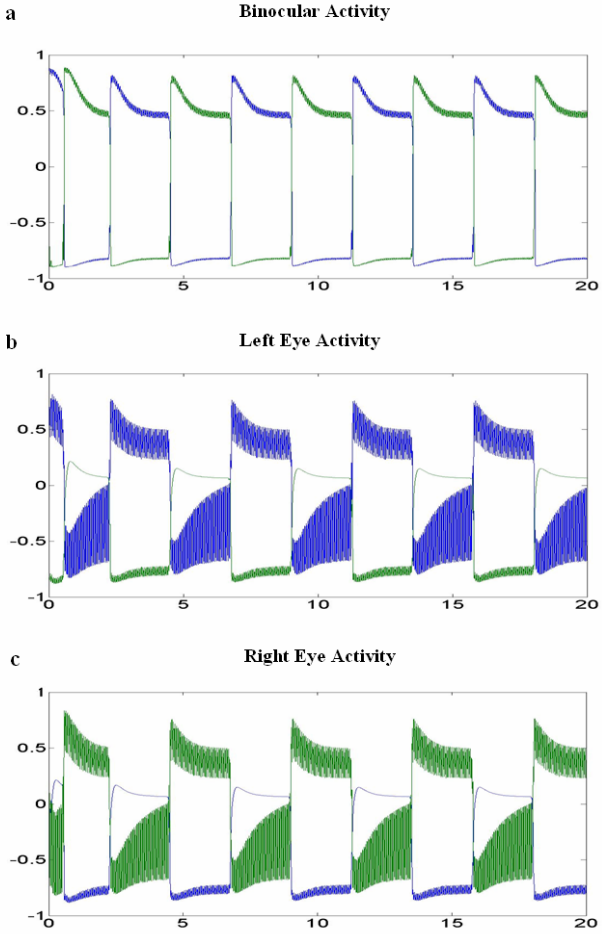

Figure 8. The model was simulated with orthogonal monocular gratings that were flickered on and off at 18 Hz. Mathematically, they are defined by $I_1^L(t) = C\left(1 - \mathrm{mod}(\lfloor 36t \rfloor, 2)\right)$, $I_2^R(t) = I_1^L(t)$, and $I_2^L(t) = I_1^R(t) = 0$, with k = 1 standing for the horizontal orientation and k = 2 standing for the vertical orientation. In particular, term $\left(1 - \mathrm{mod}(\lfloor 36t \rfloor, 2)\right)$ denotes the flickering on and off at 18 Hz, mod(a,b) is the remainder after division of integer a by integer b, $\lfloor x \rfloor$ is the highest integer less than or equal to *x*, and contrast $C = 5$. The simulation illustrates model dynamics during non-reversal trials, in which the orientations of stimuli remained unchanged in each eye throughout the trial. Green represents the model neural responses to vertical gratings, and blue represents the responses to

horizontal gratings. (a) Binocular cell activities; (b) Left monocular cell activities; (c) Right monocular cell activities.

Model simulations give the same results as these experimental data. As in the experiment of Logothetis et al (1996), the model inputs were orthogonal monocular gratings that were flickered on and off at 18 Hz. Figure 8 shows the simulation results for non-reversal trials, in which the orientations of stimuli remained unchanged in each eye (vertical grating to right eye, horizontal grating to left eye) throughout the trial. The binocular cells track the left and right eye inputs to them. Figure 9 shows the result for reversal trials, in which the flickering gratings were exchanged between the two eyes every 333 ms. The simulations show that the model exhibits the same dynamics as the experiment data of Logothetis et al (1996). The dominance duration is almost the same in both conditions (binocular cells in Figures 8a and 9a), at about 2.3s and spanning about seven swaps (monocular cells in Figures 9b and 9c).

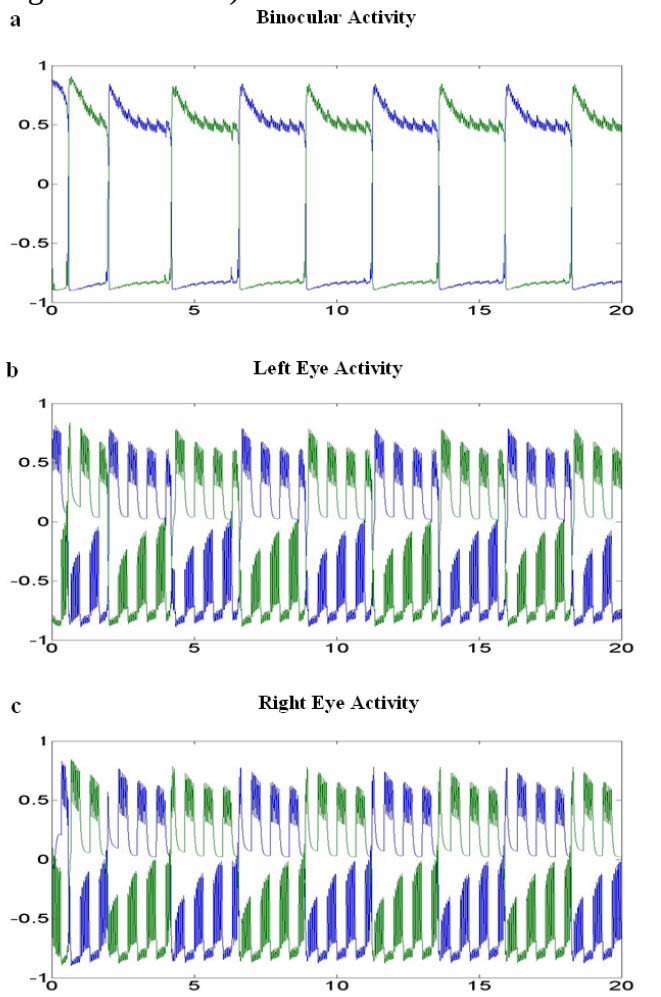

Figure 9. Simulation result for reversal trials, in which the flickering gratings were exchanged between the two eyes every 333 ms. Mathematically, they are defined by $I_1^L(t) = 5(1 - \mathrm{mod}(\lfloor 3t \rfloor, 2))(1 - \mathrm{mod}(\lfloor 36t \rfloor, 2))$, $I_2^L(t) = 5\,\mathrm{mod}(\lfloor 3t \rfloor, 2)(1 - \mathrm{mod}(\lfloor 36t \rfloor, 2))$, $I_1^R(t) = I_2^L(t)$, and $I_2^R(t) = I_1^L(t)$, with k

= 1 standing for the horizontal orientation and k = 2. In particular, term $(1-\mathrm{mod}(\lfloor 3t \rfloor,2))$ denotes the swap between the two eyes every 333 ms (or 1.5 Hz), and hence term $(1-\mathrm{mod}(\lfloor 3t \rfloor,2))(1-\mathrm{mod}(\lfloor 36t \rfloor,2))$ denotes the flickering gratings were exchanged between the two eyes every 333 ms. The result is the same as in the experimental data of Logothetis et al (1996). (a) Binocular cell activities; (b) Left monocular cell activities; (c) Right monocular cell activities. See text for details.

In the next simulation, as in the experiment of Lee and Blake (1999), we doubled the stimulus contrast of the grating stimuli and presented them at a slower swapping rate. The simulation result is shown in Figure 10. Here, rapid eye rivalry alternations occur in the binocular cells (Figure 10a), rather than the slow, irregular changes that are characteristic of stimulus rivalry (Figure 9a).

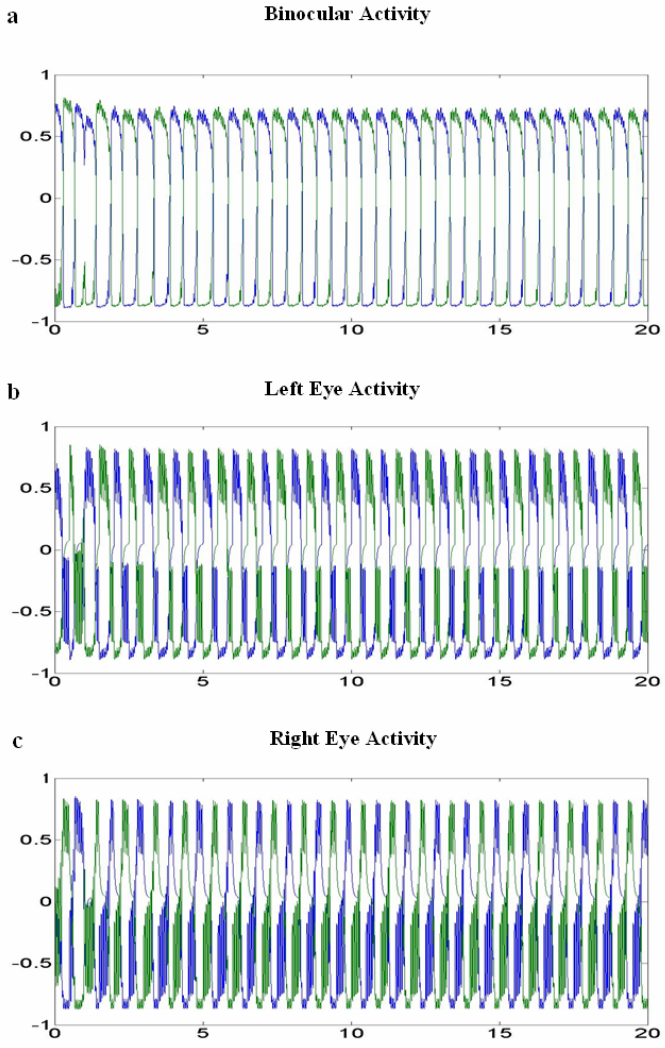

Figure 10. Simulation result for reversal trials with stimulus contrast (10) twice as high as that in Figure 9 and slow swapping (swapping at every 500ms):

$I_1^L(t) = 10(1 - \mathrm{mod}(\lfloor 2t \rfloor, 2))(1 - \mathrm{mod}(\lfloor 36t \rfloor, 2))$,

$I_2^L(t) = 10\,\mathrm{mod}(\lfloor 2t \rfloor, 2)(1 - \mathrm{mod}(\lfloor 36t \rfloor, 2))$, $I_1^R(t) = I_2^L(t)$, and $I_2^R(t) = I_1^L(t)$, with k = 1 standing for the horizontal orientation and k = 2.. The result is consistent with the Lee and Blake (1999) experimental data. (a) Binocular cell activities;(b) Left monocular cell activities; (c) Right monocular cell activities. See text for details.

How does the 3D LAMINART model (Figure 2) generate these results? The model includes both monocular cells within layers 6-to-4 of V1 and binocular grouping cells within V2. The V2 binocular grouping cells in layer 2/3 receive inputs from V2 layer 4 cells which sum all monocular and binocular inputs from V1. The bottom-up monocular pathways in layers 6-to-4 of V1 can also be modulated by feedback from binocular groupings in V2 layer 2/3 that reach V1 layer 6 and then propagate up to V1 layer 4. Both intraocular orientational competition within V1 monocular channels and interocular competition between V1 monocular channels occur, where eye rivalry can be originated. (See Grossberg and Howe (2003) and Grossberg and Raizada (2000) for reviews of supportive anatomical data.)

The coexistence of stimulus rivalry and eye rivalry may be intuitively explained as follows. When a vertical grating in the left eye wins, its excitatory habituative transmitter gate will deplete, while the excitatory habituative transmitter gate of the losing horizontal grating accumulates. Slow swapping allows the habituative transmitter depletion and accumulation processes to progress sufficiently between swaps. When, for example, a swap from a vertical grating to a horizontal grating in the left eye occurs, then the horizontal grating can win quickly because of its accumulated habituative transmitter value. A high contrast can greatly enhance this process, because the habituation rate is activity-dependent, as occurs during rapid “eye rivalry”. On the other hand, when a swap is too fast, the habituative transmitters cannot deplete and accumulate sufficiently between swaps, so that the swap cannot make the opposite grating win. As a result, it looks like the swap never happened. This generates the slow “stimulus rivalry” case. A low contrast will help the slow “stimulus rivalry” process by further slowing the rate of transmitter depletion and accumulation.

In general, these properties of habituative transmitters clarify how the brain *resets* cortical representations in response to changing perceptual stimuli. Binocular rivalry is just one case of such a reset phenomenon. Another case where the sensitivity of habituation rate to stimulus contrast plays a role is visual persistence (e.g., Bowen, Pola, and Matin, 1974; Meyer, Lawson, and Cohen, 1975; Meyer and Ming, 1988), many properties of which can also be quantitatively explained by a combination of bipole grouping, orientational competition, and habituative transmitters (Francis and Grossberg, 1996; Francis, Grossberg, and Mingolla, 1994).

These simple ideas clarify how both stimulus rivalry and eye rivalry can both occur in the model in Figure 2. It is, however, too complicated to simulate this complete multilayer network with feedback. In order to make the simulations more manageable, we have instead simulated a lumped model which includes the rate-limiting processes that drive these percepts. See Appendix equations (10) – (19) for the mathematical definition of this lumped model.

The model explanation of how stimulus rivalry and eye rivalry can coexist is consistent with data showing that, for stimuli rapidly swapped between the eyes, rivalry

shifts gradually from eye rivalry to stimulus, or pattern, rivalry when pattern coherence, as reflected by properties such as texture uniformity and contour smoothness, is increased (Bonneh and Sagi, 1999; Bonneh, Sagi, and Karni, 2001). More generally, such data support the prediction that perceptual grouping plays a key role in binocular rivalry, just as it does in explaining many data about normal non-rivalrous 3-D vision within the 3D LAMINART model and its precursors (Cao and Grossberg, 2005; Grossberg, 1987, 1994; Grossberg and McLoughlin, 1997; Grossberg and Swaminathan, 2004; Grossberg and Yazdanbaksh, 2005).

Qualitative Explanations of Other Binocular Rivalry Data

This section summarizes how the 3D LAMINART model can qualitatively explain other types of data about binocular rivalry.

Modulation of primary visual cortex activity with binocular rivalry. Why does neuronal activity in human primary visual cortex correlate with perception during binocular rivalry (Polonsky et al., 2000), and is ~ 55% as large as that evoked by alternately presenting two monocular images without rivalry? As shown in Figure 2a, a winning grouping in layer 2/3 of V2 propagates to V2 layer 6, and then to V1 layer 6, where it modulates the excitatory activity of V1 layer 4, while inhibiting the activity of nearby V1 cells that are not supported by the perceived orientation. Modulating matched inputs while strongly inhibiting mismatched inputs clarifies why activity modulation in the rivalry condition is ~55% as large as the responses that are evoked by alternately presenting the two monocular images without rivalry, since alternating presentation eliminates the inhibitory off-surround suppression. This qualitative explanation is consistent with quantitative simulations (Grossberg and Raizada, 2000) of neurophysiological data concerning how top-down attention from V2 can modulate the strength of perceptual groupings in V1 (Roelfsema, Lamme, and Spekreijse, 1998).

Effects of object attention on switching between superimposed transparent surfaces. Mitchell, Stoner, and Reynolds (2004) cued attention to one of two superimposed transparent surfaces and then deleted the image of one surface from each eye, resulting in rivalry in which the cued surface dominated. An explanation of these data is facilitated by modeling results of Grossberg and Yazdanbakhsh (2005), who used the 3D LAMINART model to simulate data about 3-D percepts of transparent surfaces, including percepts of bistable transparency. In particular, this study simulated how top-down attention can bias which surface will be seen as the nearer transparent figure, and drive the percept of the other surface to the further background. Grossberg and Yazdanbakhsh did not include habituative transmitters to make these bistable percepts spontaneously oscillate. However, Grossberg and Swaminathan (2004) did include habituative transmitters in their study, which explained how, just as during bistable transparency, attended parts of the Necker cube look closer. By including habituative transmitters, their simulations could also show how the 2-D Necker cube stimulus can induce bistable 3-D cube percepts. The Mitchell et al. (2004) data can be qualitatively understood by applying the Grossberg and Swaminathan (2004) explanation to the case of transparency-inducing stimuli.

How does attentional feedback influence a visible surface percept? Suppose for definiteness that spatial attentional feedback from higher cortical levels causes greater

activation of the monocular surface representations in the V2 thin stripes (see Figure 2b). This enhancement can strengthen the corresponding boundary grouping in the V2 pale stripes via surface-to-boundary signals, thereby enhancing the competitive advantage of this grouping during rivalry (Figure 2a). The result of this rivalrous boundary competition is seen in the surface percept after boundary-to-surface signaling selects the surface of the winning boundary in V2 via surface capture, and then propagates this result to the visible binocular surface percept in V4 (Figure 2b). This qualitative explanation is supported by quantitative data simulations that use the same model mechanisms, but in response to different perceptual stimuli, in Fang and Grossberg (2007), who simulate 3-D surface percepts that are derived from stereograms; and in Grossberg and Yazdanbakhsh (2005), who simulate 3-D surface percepts of transparency and neon color spreading.

Monocular Rivalry. Monocular rivalry occurs when a grid that is presented to one eye breaks down into individual oriented components that compete for visibility in a manner that shares some properties of what happens during binocular rivalry (Breese, 1899; Campbell and Howell, 1972; Maier, Logothetis, and Leopold, 2005; Sindermann and Lueddeke, 1972). The properties of monocular rivalry, when compared with those of binocular rivalry, provide further support for the model circuits in Figure 2, notably for: the role of boundary completion during perceptual grouping; the prediction that all boundaries are invisible; and the manner in which percepts are rendered visible due to boundary-mediated capture and filling-in of surface lightness and color.

In particular, both monocular rivalry and binocular rivalry properties (e.g., rates) increase monotonically with the orientational difference in the rivalrous patterns (Campbell et al., 1973; O'Shea, 1998; Wade, 1975). This result is consistent with the idea that orientational competition influences both types of rivalry. Orientational competition, with maximal strength at orthogonal orientations, is an important property of perceptual grouping. Orientational competition can occur at several stages of the perceptual grouping process to carry out different functional roles. For example, it can prevent lightness and color from flowing out of line ends and other object contour locations that undergo an abrupt change of orientation, and it can help to select the grouping whose orientation has the most perceptual evidence (Grossberg, 1994; Grossberg and Mingolla, 1985).

Monocular and binocular rivalry also differ in various ways. For example, the rate of monocular rivalry is less than that for binocular rivalry at essentially every orientational difference. Binocular rivalry is typically also much crisper and easier to report than monocular rivalry. Various authors have attributed these properties to the contribution of a "cooperative process that produces global activity fluctuations…coherent stimuli initiate global transitions, which may involve large cortical networks across both hemispheres" (Bonneh, Sagi, and Karni, 2001, p. 987). Our model predicts that a key organizer of this global process is the perceptual grouping circuitry in layer 2/3 of the pale stripes of cortical area V2.

In addition, the binocular rivalry rate is much greater between near-horizontal stimuli than between near-vertical stimuli, and this difference disappears at large orientation differences. In contrast, there is no such pattern of results for monocular rivalry. O'Shea (1998) proposed the following explanation of this difference in the results for monocular and binocular rivalry: Near-vertical gratings presented to opposite eyes engage stereopsis, and a single grating is seen tilted in depth (Wheatstone, 1838/1952).

Stereopsis appears to inhibit binocular rivalry (Blake and Boothroyd, 1985). These observations are consistent with FACADE and 3D LAMINART mechanisms for how binocularly fused 3-D perceptual grouping and perception occurs (Figure 2). In particular, these models clarify how binocular fusion can free the left and right eye images from the competitive interactions that could otherwise induce rivalry. The main thing to understand is how interactions between cooperative and competitive interactions help both to select the perceptual groupings that support normal, non-rivalrous percepts, and also to generate rivalrous percepts. The basic idea that the current model explicates was proposed in Grossberg (1987, p. 122, see Figure 6; 1994, p. 103, see Figure 41); namely, binocular fusion at V1 complex cells enables these cells to input to the on-center of the layer 6-to-4 modulatory on-center, off-surround circuit in V2 (Figure 2a) and from there to be incorporated into non-rivalrous perceptual groupings in V2 layer 2/3. In contrast, the failure of left and right eye inputs to fuse in V1 causes their V1 complex cell outputs to compete within their V2 layer 6-to-4 off-surrounds, thereby initiating rivalry of their respective V2 layer 2/3 perceptual groupings.

A compelling example of how perceptual grouping contributes to monocular rivalry was described by Maier, Logothetis, and Leopold (2005). They constructed stimuli in which a central portion contains a non-rivalrous pattern (e.g., vertical bars) but the surrounding image contains a rivalrous pattern (e.g., a grating of horizontal and vertical bars). Were rivalry just a matter of local competition, then as one or another orientation won in the periphery, the central vertical bars should persist in their visibility. Instead, the central region of vertical bars became perceptually invisible when the horizontal bars won in the periphery. This percept can be explained by the following properties:

When the horizontal bars win, they can collinearly group across the central region. This hypothesis is consistent with the fact that suppression of the vertical bars depended upon there being strict continuity in the pattern between the unambiguous window and the surrounding rivalrous regions. The completed horizontal boundaries can inhibit the vertical boundaries in the central region via orientational competition (Figures 1 and 2a). When the vertical boundaries are inhibited, they can no longer capture the vertically oriented lightness or color signals whose surface filling-in is the basis for consciously seeing the vertical bars (Figure 2b). Hence, the vertical bars disappear. The horizontal boundaries are not seen because they are invisible, or amodal (Figure 3a). They can only become visible if they are positionally and orientationally aligned with lightness or color inducers, whose surface filling-in they would then trigger to generate a visible surface percept. However, when the winning boundaries are horizontal within the central region, they are not aligned with the lightness or color inducers of the vertical bars in the image. Hence the completed horizontal boundaries are not seen in the central region.

The above explanation follows that in Grossberg (1987, 1994) of how rivalry occurs through selection of winning oriented boundary groupings through positional and orientational competition, followed by the capture by these groupings of positionally and orientationally consistent patterns of lightnesses and colors to generate a consciously visible surface percept. Lightness and color patterns that are not consistent with winning boundaries are suppressed by double-opponent interactions that occur after surface filling-in of opponent lightnesses or colors. See Grossberg and Swaminathan (2004),

Grossberg and Yazdanbakhsh (2005), and Kelly and Grossberg (2000) for simulations of related 3-D surface percepts that depend upon the same explanation of how 3-D surface capture occurs.

Maier, Logothetis, and Leopold (2005) discussed these intriguing results in terms of "the brain's global interpretive assumptions regarding the composition of the stimulus" (p. 668). We would argue instead that they may be explained by basic properties of boundary completion and depth-selective surface capture, leading to selective filling-in of visible surface percepts. No "global interpretive assumptions" are needed to explain the basic percept. Maier, Logothetis, and Leopold (2005) also remarked that suppression of the vertical bars "generally was not accompanied by completion phenomena, such as a 'filling-in' of the horizontal bars, although faint illusory horizontal lines were reported by some subjects" (pp. 670-671). We would argue instead that boundaries are typically invisible, or amodal (Figure 3a). A visible filled-in surface percept occurs only when boundary and surface inducers are positionally and orientationally consistent. The fact that sometimes a faint horizontal boundary could be seen indicates that boundary completion did occur, but that conditions for visible surface filling-in were poor, as occurs whenever boundary and surface inducers are not aligned during rivalry.

Maier, Logothetis, and Leopold (2005) also carried out a number of other ingenious manipulations. Each of these manipulations probes the brain's circuitry for 3-D vision and figure-ground perception in a different way. An explanation of these effects will be provided in a subsequent study.

Percepts of Marroquin patterns. Wilson, Krupa, and Wilkinson (2000) have described a model of monocular rivalry that includes spatial interactions. A Marroquin pattern is produced by superimposing three copies of a square dot grid, each copy rotated by 60° relative to the others. This stimulus generates a percept of circular shapes that appear and vanish at various locations in an oscillatory fashion. Wilson et al. (2000) used orientation-selective cortical cells, their lateral interactions, and adaptation to explain the perceptual oscillation of the Marroquin patterns. In order to explain the perceived circular shape, they assumed that cells exist in V4 which selectively respond to concentric input patterns. In particular, their model uses oriented filtering, full-wave rectification and orthogonal oriented filtering (cf., Grossberg and Mingolla, 1985) to extract local curvature information from the stimulus. Then a concentric, linear summation stage produces inputs to V4 cells. As a result, these V4 cells selectively respond to circular patterns, but do not generate a perceptual representation of them. Finally, inhibitory interactions and adaptation occur between these V4 cells in order to generate oscillations.

The Wilson et al. (2000) model contains no perceptual grouping and no spatially distributed circular perceptual representation. It also cannot explain how rivalrous oscillations are generated in cortical areas V1 and V2. In our model, circular shapes are formed naturally by perceptual grouping in V2. For example, Gove, Grossberg and Mingolla (1995) simulated how model bipole cells in V2 can complete concentric illusory contours as emergent properties of model interactions. Therefore, it is not necessary to assume pre-existing concentric units. With synaptic habituation added to the perceptual grouping and competitive interactions of Gove et al. (1995), such dynamically oscillating circles will be generated in the V2 circuits of the 3D LAMINART model, rather than in V4, just like other bistable grouping representations.

The spread of suppression and binocular rivalry. Kaufman (1963) showed one horizontal line in one eye and two vertical lines in the other eye. Under dichoptic viewing, there are moments in which a halo appeared at each line intersection, and a short segment of horizontal line can be seen between the two halos, unless the spacing between the two vertical lines is too close. The 3D LAMINART model contains bipole grouping and orientation competition over a spatially extended region. The strength of spatial competition decreases with distance, which can be approximated by a Gaussian function (see equations (1) and (7) below). This explains why two halos are seen centered at the two intersections where inhibition is maximal. When the two vertical lines are far enough apart, the short segment of horizontal line in the middle of two vertical lines receives no or little inhibition, so that a short horizontal segment is seen between the two halos.

Dichoptic plaids and binocular summation. Liu et al (1992) showed that, when orthogonal gratings are viewed dichoptically at low contrast, a stable summation between the two images is perceived in the form of a dichoptic plaid. They proposed that there exists a neural process that performs a summation of dissimilar images, which is distinct from the competitive process of binocular rivalry and suppression. The 3D LAMINART model contains such a summation neural process. In it, binocular cells in V2 layer 4 sum both monocular information from both eyes as well as binocularly fused information from V1 layer 2/3 (see Figure 2a). This neural process has been used to explain and quantitatively simulate data about da Vinci stereopsis (Cao and Grossberg, 2005; Grossberg and Howe, 2003), among other data about stereopsis.

When two orthogonal gratings are viewed dichoptically, there is no binocular fusion in V1 layer 3B. Therefore, cells in the pale stripes of V2 layer 4 only sum monocular boundary information from both eyes. At low contrast, orientational competition from orthogonal gratings is reduced and hence neither orientation can gain dominance. As a result, V2 boundary cells that code both orientations can remain simultaneously active and support a stable surface percept of a dichoptic plaid. Unlike the hypotheis of Liu et al. (1992), however, the 3D LAMINART model does not require a distinct neural process for binocular summation. Instead, the model uses a unified neural architecture (Figure 2) to explain binocular fusion, rivalry, and summation.

Fusion of dichoptic gratings. Burke et al (1999) presented multiple parallel lines with a high contrast to each eye. The parallel lines shown to one eye were perpendicular to those presented to the other eye. In condition (a), neither of parallel lines had gaps, but in conditions (b), (c), and (d), there were gaps in horizontal lines, vertical lines, or both at the dichoptic intersection zones, respectively. The subject reported the highest incidence of the “no” disappearance, or non-rival mixture of vertical and horizontal lines, in condition (d), and less so in conditions (b) and (c). The incidence of rival disappearance was highest in condition (a) in which none of the parallel lines had gaps. The finding is quite notable with respect to the model grouping and orientational competition processes. The reduction of orientational competition in condition (d) is maximal due to the binocular presence of the gaps, and less in conditions (b) and (c) because the gaps are monocular. In (a), the lack of the gaps maximally activates the orientational competition, hence induces the highest incidence of rivalry. Bipole grouping and orientational competition with spatial extent can hereby qualitatively explain these results.

General suppression during binocular rivalry. As noted above, a number of psychophysical experiments have shown that binocular rivalry displays produce a general

suppression that is not feature specific; e.g., Blake and Fox (1974), Blake and Lema (1978), and Wales and Fox, 1970). How does the 3D LAMINART model account for such data? Why is not orientational competition more selective in what it suppresses? Grossberg (1987) qualitatively explained such general suppression data by invoking two model mechanisms that are consistent with the present analysis.

The first type of model mechanism occurs within the boundary processing stream: Orientational competition itself does not just suppress orthogonal orientations; it suppresses all orientations that deviate sufficiently from the winning orientation. See Appendix equation (7). The second type of model mechanism concerns the way in which boundaries capture surface lightnesses and colors: If a spatial pattern of lightness or color has a different orientation or position from the capturing boundary, then it will be suppressed by double-opponent interactions within the corresponding lightness and color filling-in domains (see Grossberg (1987), Sections 26 and 27).

Pattern rivalry of concentric rings and spokes. The 3D LAMINART model can also qualitatively explain the rivalrous percept of a dichoptic display where a set of concentric rings is shown in one eye and a set of spokes is shown in the other eye. When viewed dichoptically, the rings and the spokes are engaged in robust rivalry. In particular, when there are 8 or 16 spokes, the rings as a pattern are suppressed by the spokes as a pattern, and vice versa. This percept may be explained as follows:

The 3D LAMINART model contains both boundary and surface processes (Figure 2). The boundary and surface cortical streams obey complementary laws (Figure 3) and interact with each other to overcome their complementary deficiencies and to create a consistent percept. Surfaces are formed via a surface filling-in process. Boundaries act both as filling-in inducers and filling-in barriers. Closed boundaries can contain filling-in of surface regions that can enter 3-D percepts, but boundaries with sufficiently big gaps in them cannot (Cao and Grossberg, 2005; Grossberg, 1994; Grossberg and Howe, 2003; Grossberg and Yazdanbakhsh, 2005). The surfaces that successfully contain filling-in generate contour-sensitive surface-to-boundary signals that ensure that the boundary and surface representations are consistent (see Figure 2b). This process strengthens the boundaries that generated these surfaces, while suppressing redundant boundaries. Surface-to-boundary feedback also initiated figure-ground separation of objects from one another and from their backgrounds.

The surface-to-boundary feedback process also clarifies how the rings and spokes can rival as patterns. In particular, a broken boundary enables nearby surface filling-in signals to flow out, and therefore weakens the corresponding surface representation and its surface-to-boundary feedback signals. When a ring boundary is broken by orientational competition at enough intersections with a spoke boundary, it will receive weak or no surface-to-boundary feedback signals. As a result, the broken ring boundary is not strengthened, but the unbroken spoke boundaries are. This helps the other spokes to win over the ring at other positions of the image. In addition, the colinear grouping process along a single spoke makes that spoke stronger due to less inhibition in the broken area of the ring, and hence helps to suppress the other rings. As a result, the ring as a pattern may be suppressed by the spokes as a pattern. This argument also clarifies how the rings can win over the spokes.

Discussion

The 3D LAMINART model predicts that rivalry is driven by three interacting properties of binocular perceptual grouping circuits in layer 2/3 of V2: bipole grouping, orientational competition, and habituative or depressing synapses. A strong prediction of the model is that direct cortical stimulation of layer 2/3 of V2 which alters the strength or timing of bipole grouping via recurrent excitatory connections should also alter the strength or timing of rivalry percepts. In particular, stimulation that persistently strengthens one orientation over another may be able to terminate a rivalry percept entirely. The full model qualitatively clarifies rivalry properties in many brain regions as manifestations of how the brain generates 3-D boundary and surface percepts using intracortical and interstream feedback processes, and attends to salient visual information using top-down intercortical feedback processes. The model hereby quantitatively explains and simulates a wide range of data about binocular rivalry (see Table 1; Lee and Blake, 1999; Levelt, 1967; Logothetis at al., 1996; Muller and Blake, 1989; Ngo et al., 2000; Polonsky et al., 2000), and qualitatively explains a much larger data base about monocular and binocular rivalry, using a cortical model of 3-D vision that was developed to explain data about non-rivalrous perception. The result is a functional and mechanistic explanation of how rivalry phenomena arise from basic cortical mechanisms of non-rivalrous 3-D vision. With this foundation, it is now possible to further develop, analyze, and test a model in which both non-rivalrous and rivalrous percepts are caused by the same set of cortical mechanisms in response to different visual stimuli.

Appendix A. Binocular Grouping Equations

The 3D LAMINART model does not restrict the number of cells and their orientations, and can hence be implemented to process complex natural scenes (e.g., Mingolla, Ross, and Grossberg, 1999). In order to reduce the computational cost of our simulations, and to exhibit key properties in the simplest way, we used a 15x15 grid of 225 V2 layer 2/3 horizontal pyramidal cells, and the same number of vertical pyramidal cells. For each pyramidal cell, there are two di-synaptic inhibitory interneurons. There were also 255 equations for excitatory and inhibitory habituative transmitters, respectively. The forward Euler method was used in the simulations.

Binocular Cell Activities (V2). As shown in Figure 1a, bipole grouping in the model is achieved by an interaction of long-range monosynaptic excitation and shorter-range di-synaptic inhibition that together converge on pyramidal cells in the pale stripes of cortical area V2. The bipole pyramidal cells interact recurrently in this grouping network via their long-range monosynaptic connections, as do the di-synaptic inhibitory interneurons via their shorter-range inhibitory connections. Binocular cell activity, x_{ijk}, of such a bipole grouping cell at position (i,j) and orientation k is defined by the following membrane, or shunting, equation:

$$\frac{d}{dt}x_{ijk} = -x_{ijk} + (1-x_{ijk})h^{+}_{ijk}\left(\gamma\left([H^{1}_{ijk} + I_{ijk} + H^{2}_{ijk} - H^{I}_{ijk}]^{+} + [x_{ijk}]^{+}\right)\right) - (1+x_{ijk})\eta\left[O_{ijk}\right]^{+}, \quad (1)$$

where the excitatory input $\left([H^{1}_{ijk} + I_{ijk} + H^{2}_{ijk} - H^{I}_{ijk}]^{+} + [x_{ijk}]^{+}\right)$ is gated by h^{+}_{ijk}, the excitatory habituative transmitter gate (Figures 1d and 1e), which is defined in (8). The excitatory and inhibitory gain parameters $\gamma = 0.07$ and $\eta = 1.1$.

The excitatory input describes the effects of bottom-up inputs I_{ijk} and the long-range horizontal connections $H^{1}_{ijk} + H^{2}_{ijk} - H^{I}_{ijk}$ that support perceptual grouping. The bottom-up oriented input I_{ijk} comes from lower cortical layers. It is an increasing function of contrast. See the figure captions for how the inputs were defined. In the simulations, horizontal (k=1) and vertical orientations (k=2) are used. The horizontal bottom-up input I_{ij1} is fixed as a constant (15), while the vertical bottom-up input I_{ij2} varies (from 15.5 to 17.5).

Long-Range Excitatory Connections. Terms H^{1}_{ijk} and H^{2}_{ijk} in (1) describe excitatory inputs from long-range connections, as part of the bipole grouping process:

$$H^{u}_{ijk} = \sum_{pq} W_{pqijku}[x_{ijk}]^{+}, \quad (2)$$

where W_{pqijku} are the long-range connection weights from cells at position (p,q) and orientation k on either side (u = 1 or u = 2) to the target cell at position (i,j) and orientation k. The weights for a horizontally oriented cell are defined by spatially elongated Gaussian kernels:

$$W_{pqij11} = \left[sign(i-p) \exp\left(-\left(\frac{(i-p)^2}{\sigma_p^2} + \frac{(j-q)^2}{\sigma_q^2} \right) \right) \right]^+, \quad (3)$$

and

$$W_{pqij12} = \left[sign(p-i) \exp\left(-\left(\frac{(i-p)^2}{\sigma_p^2} + \frac{(j-q)^2}{\sigma_q^2} \right) \right) \right]^+, \quad (4)$$

where $sign(w)$ equals +1 if $w \geq 0$ and 0 if $w < 0$, and parameters σ_p and σ_q equal 6 and 0.3, respectively. The kernel weights for the vertical orientation are obtained by rotating the horizontal kernel by 90 degrees.

Short-Range Inhibitory Interneurons. Term H_{ijk}^I in (1) is the inhibitory input from di-synaptic inhibitory interneurons on both sides of the target pyramidal cell. As noted above, the net input from the excitatory long-range inputs and the di-synaptic inhibitory inputs define the bipole property that controls perceptual grouping. Term H_{ijk}^I is defined by summing inputs from the left and right inhibitory interneurons at each position and orientation:

$$H_{ijk}^I = \beta([s_{ijk1}]^+ + [s_{ijk2}]^+), \quad (5)$$

where β is a constant (0.2), and s_{ijk1} and s_{ijk2} are the left and right inhibitory interneuron activities. Each inhibitory interneuron (or neuronal population) is activated by the long-range excitatory input on the corresponding side of the target pyramidal cell (see Figure 1a). In addition, the pair of inhibitory interneurons corresponding to a given bipole pyramidal cell mutually inhibit one another by shunting inhibition. This shunting inhibition tends to normalize the total activity of the inhibitory pair, and enables the bipole cell to fire if it receives excitation from both sides (two excitatory inputs against one inhibitory one), but not if it receives excitation from only one side (one excitatory input against one inhibitory one, since the total inhibition is normalized). This interaction between long-range excitation and recurrent shunting inhibition is described by:

$$\frac{d}{dt} s_{ijku} = \delta\left(-s_{ijku} + H_{ijk}^u - s_{ijku}[s_{ijkv}]^+ \right), \quad (u, v = 1,2, \quad u \neq v) \quad (6)$$

where δ is a constant (3).

The inhibitory input term O_{ijk} in (1) is due to orientational competition within a spatial region, described by:

$$O_{ijk} = \sum_{pq, r \neq k} h_{ijk}^- [x_{pqr}]^+ \exp\left(-\left(\frac{(i-p)^2}{\sigma_p^2} + \frac{(j-q)^2}{\sigma_p^2} \right) \right), \quad (7)$$

where h_{ijk}^- is the inhibitory habituative transmitter associated with the cell, and parameters σ_p and σ_q both equal 5.

Habituative Transmitter Gates. Excitatory (h_{ijk}^+) and inhibitory (h_{ijk}^-) habituative transmitters are defined by:

$$\frac{d}{dt}h_{ijk}^{+} = (1 - h_{ijk}^{+}) - B_h^{+} h_{ijk}^{+}[x_{ijk}]^{+} + s(t), \quad (8)$$

and

$$\frac{d}{dt}h_{ijk}^{-} = (1 - h_{ijk}^{-}) - B_h^{-} h_{ijk}^{-}[O_{ijk}]^{+} + s(t). \quad (9)$$

(Grossberg, 1972, 1980). These processes describe transmitter accumulation to a constant maximum of 1 via the terms (1-h) and gated habituation, inactivation, or depression by the $h[x]^{+}$ and $h[O]^{+}$ terms. Constants B_h^{+} and B_h^{-} equal 10 and 8 respectively, and *s(t)* is a uniformly distributed random number within the interval (-0.15, 0.35) which incorporates cellular noise into the network in a simple way. Habituation sets the stage for rivalry by weakening an active grouping in an activity-dependent way, as in equation (1). However, habituation, by itself, does not cause rivalry. It has been known for a long time (e.g., Grossberg, 1972, 1980; Grossberg and Seidman, 2006) that habituation can cause an overshoot in a cell's initial response followed by a gradual decline to a steady-state value. This steady-state value is an increasing function of input intensity. Thus, in the absence of orientational competition, a grouping can approach a stable equilibrium after undergoing an initial transient of enhanced activation. In the present model, the simulation that is summarized in Figure 7 shows that, in fact, the model converges to a stable equilibrium in response to horizontal inputs to both eyes, even though the same system, with the same parameters, undergoes rivalry when horizontal inputs are presented to one eye and vertical inputs to the other eye. See Francis (1996, 1997), Francis and Grossberg (1996), and Francis, Grossberg, and Mingolla (2004) for simulations of other types of data where grouping and habituation occur without causing rivalry.

Appendix B. Lumped Model Equations

As summarized in Figure 2, the 3D LAMINART model includes both monocular cells within layers 6-to-4 of V1 and binocular grouping cells within V2. The outputs from these monocular and binocular cells are summed at V2 layer 4 cells which, in turn, send them to the V2 binocular bipole grouping cells in V2 layer 2/3. The bottom-up monocular pathways in layers 6-to-4 of V1 can also be modulated by feedback from binocular groupings in V2 layer 2/3 that reach V1 layer 6 and then propagate up to V1 layer 4. There is intraocular orientational competition within V1 monocular channels and interocular orientational competition between V1 monocular channels, where eye rivalry can occur. Due to the complexity of the complete model, the spatially distributed activities x_{ijk} in Appendix A with positional indices (i,j) and orientations k were simulated here as spatially lumped variables x_k^m , one for each eye (m = L for left, and R for right) and two perpendicular orientations (k = 1, 2, with 1 standing for horizontal and 2 for vertical). The lumped variables x_k^L , x_k^R , and x_k^B below thus represent cell activities of the k^{th} Left monocular channel in V1, the k^{th} Right monocular channel in V1, and the k^{th} binocular channel in V2, respectively.

Monocular Cell Activities (V1)

Each monocular V1 cell obeys a shunting, or membrane equation. Its net activity is determined by a bottom-up excitatory input, recurrent excitation from its own output,

activity-dependent habituation in response to both of these monocular excitatory inputs, top-down excitatory feedback from the corresponding V2 binocular cell, orientational competition from the perpendicular orientation corresponding to its own eye, and weaker orientational competition from the perpendicular orientation of the other eye. In all,

$$\tau \frac{d}{dt} x_k^L = -x_k^L + (1 - x_k^L) h_k^{L,+} (\gamma (I_k^L + \left[x_k^L \right]^+) + \mu \left[x_k^B \right]^+) - (1 + x_k^L) O_k^L , \quad (10)$$

$$\tau \frac{d}{dt} x_k^R = -x_k^R + (1 - x_k^R) h_k^{R,+} (\gamma (I_k^R + \left[x_k^R \right]^+) + \mu \left[x_k^B \right]^+) - (1 + x_k^R) O_k^R , \quad (11)$$

where $h_k^{L,+}$ and $h_k^{R,+}$ are habituative transmitters of the monocular left and right eye cells, respectively; I_k^L and I_k^R are contrast-sensitive inputs; x_k^B represents feedback from the corresponding binocular cell; and O_k^L and O_k^R represent orientational competition from both interocular and intraocular monocular V1 cells:

$$O_k^L = \alpha \left[x_r^R \right]^+ + \beta \left[x_r^L \right]^+ , \quad (12)$$

$$O_k^R = \alpha \left[x_r^L \right]^+ + \beta \left[x_r^R \right]^+ , \quad (13)$$

where $k, r = 1,2$ and $r \neq k$.

Binocular Cell Activities (V2)

Each binocular V2 cell also obeys a shunting, or membrane equation. Its net activity is determined by a bottom-up excitatory input that sums the outputs of like-oriented left and right eye monocular V1 cells, recurrent excitation from its own output, activity-dependent habituation in response to both of these binocular excitatory inputs, and orientational competition from the binocular cell corresponding to the perpendicular orientation. In all,

$$\tau \frac{d}{dt} x_k^B = -x_k^B + (1 - x_k^B) h_k^{B,+} (\gamma (I_k^B + \left[x_k^B \right]^+)) - (1 + x_k^B) O_k^B , \quad (14)$$

where $h_k^{B,+}$ is a habituative transmitter, I_k^B is a binocular input from V1 cell activities, the binocular input

$$I_k^B = \delta (\left[x_k^L \right]^+ + \left[x_k^R \right]^+) , \quad (15)$$

and O_k^B is orientational inhibition:

$$O_k^B = \eta \left[x_r^B \right]^+ , \quad (16)$$

where $k, r = 1,2$ and $r \neq k$.

Habituative Transmitter Gates

The monocular and binocular habituative transmitters obey the same type of law as in (8) and (9). A noise term was not added in the present simulations, since the gamma distribution of Figure 5 was not an explanatory target of these simulations:

$$\tau_h \frac{d}{dt} h_k^{L,+} = (1 - h_k^{L,+}) - B_h^+ h_k^{L,+} \left[x_k^L \right]^+ , \quad (17)$$

$$\tau_h \frac{d}{dt} h_k^{R,+} = (1 - h_k^{R,+}) - B_h^+ h_k^{R,+} \left[x_k^R \right]^+ , \quad (18)$$

$$\tau_h \frac{d}{dt} h_k^{B,+} = (1 - h_k^{B,+}) - B_h^+ h_k^{B,+} \left[x_k^B \right]^+ , \quad (19)$$

where $k = 1,2.$

Parameters $\tau = 0.03,\ \tau_h = 3,\ \alpha = 6,\ \beta = 8,\ \eta = 10,\ \gamma = 1,\ \mu = 0.1,\ B_h^+ = 10,$ and $\delta = 10$ in all equations. The lumped version activation equations (10), (11), and (14) have the term τ = 0.03 on the left hand side. In contrast, the corresponding activation equation (1) in the un-lumped model has the rate 1. This difference may raise the concern why the rate of activation should be scaled by 1/0.03 in the lumped model. A different rate τ_h also holds for the corresponding habituation equations (17) – (19) in the lumped model vs. equations (8) and (9) in the un-lumped model. These parameter differences compensate for the lumping of the distributed network formulation, without any conceptual change in the dynamics of the network. For example, the change in the activation parameter γ in the lumped version balances for lumping the summation $[H_{ijk}^1 + I_{ijk} + H_{ijk}^2 - H_{ijk}^I]$ of perceptual grouping terms on the right-hand side of (1).

References

Abbott, L. G., Varela, J. A., Sen, K., and Nelson, S. B. (1997). Synaptic depression and cortical gain control. Science 275, 220–224.

Arrington, K.F. (1993) Neural network models for color and brightness perception and binocular rivalry. PhD Dissertation, Boston University. *University Microfilms International, Ann Arbor, Michigan.*

Blake R. (1989). A neural theory of binocular rivalry. Psychological Review, 96, 145-167.

Blake, R., and Boothroyd, K. (1885). The precedence of binocular fusion over binocular rivalry. Perception and Psychophysics, 37, 114-124.

Blake, R., and Fox, R. (1974). Binocular rivalry suppression: Insensitive to spatial frequencey and orientation change. Vision Research, 14, 687-692.

Blake, R., and Lema, S.A. (1978). Inhibitory effect of binocular rivalry suppression is independent of orientation. Vision Research, 18, 541-544.

Blake, R., and Logothetis, N. (2002). Visual Competition. Nature Reviews Neuroscience, 3, 13-23.

Blake, R., O'Shea, R.P., and Mueller, T.J. (1992). Spatial zones of binocular rivalry in central and peripheral vision. Visual Neuroscience, 8, 469-478.

Bonneh, Y., and Sagi, D. (1999). Configuration saliency revealed in short duration binocular rivalry. Vision Research, 39, 271-291.

Bonneh, Y., Sagi, D., and Karni, A. (2001). A transition between eye and object rivalry determined by stimulus coherence. Vision Research, 41, 981-989.

Bosking, W., Zhang, Y., Schofield, B., and Fitzpatrick, D. (1997). Orientation selectivity and the arrangement of horizontal connections in tree shrew striate cortex. Journal of Neuroscience, 17, 2112–2127.

Bowen, R., Pola, J., and Matin, L. (1974). Visual persistence: Effects of flash luminance, duration and energy, Vision Research, 14, 295-303.

Breese, B. B. (1899). On inhibition. Psychological Monographs, 3, 1-65.

Burke, D., Alais, D., and Wenderoth P. (1999). Determinants of fusion of dichoptically presented orthogonal gratings. Perception, 28, 73-88.

Campbell, F.W., Gilinsky, A.S., Howell, E.R., Riggs, L.A., and Atkinson, J. (1973). The dependence of monocular rivalry on orientation. Perception, 2, 123-125.

Campbell, F. W., & Howell, E. R. (1972). Monocular alternation: A method for the investigation of pattern vision. Journal of Physiology, 225, 19P-21P.

Cao, Y., and Grossberg, S. (2005). A laminar cortical model of stereopsis and 3-D surface perception: Closure and da Vinci stereopsis. Spatial Vision, 18, 515-578

Carpenter, G.A., and Grossberg, S. (1981). Adaptation and transmitter gating in vertebrate photoreceptors. Journal of Theoretical Neurobiology 1, 1-42

Carpenter, G.A., and Grossberg, S (1990). ART 3: Hierarchical search using chemical transmitters in self-organizing pattern recognition architectures. Neural Networks, 3, 129-152.

Diaz-Caneja, E. (1928). Sur l'alternance binoculaire. Ann. Ocul. (Paris) 165, 721–731.

Dragoi, V, Rivadulla, C, and Sur, M. (2001). Foci of orientation plasticity in visual cortex. Nature, 411, 80-86.

Engel, A. K., Fries, P., & Singer, W. (2001). Dynamic predictions: Oscillations and synchrony in top-down processing. Nature Reviews Neuroscience, 2, 704 –716.

Fang, L., and Grossberg, S. (2007). From stereogram to surface: How the brain sees the world in depth. Technical Report CAS/CNS-TR-06-013. Spatial Vision, in press.

Field, D.J., Hayes, A., and Hess, R.F. (1993). Contour integration by the human visual system: evidence for a local "association field". Vision Researn, 33, 173-193.

Fox R. (1991). Binocular rivalry. In Binocular Vision and Psychophysics, D.M. Regan, ed. (MacMillan Press, London), pp. 93-110.

Fries, P., Reynolds, J.H., Rorie, A.E., and Desimone, R. (2001). Modulation of oscillatory neuronal synchronization by selective visual attention. Science, 291, 1560-1563.

Francis, G. (1996). Cortical dynamics of visual persistence and temporal integration. Perception & Psychophysics, 58, 1203-1212.

Francis, G. (1997). Cortical dynamics of lateral inhibition: Metacontrast masking. Psychological Review, 104, 572-594

Francis, G, and Grossberg, S. (1996). Cortical dynamics of boundary segmentation and reset: persistence, afterimages, and residual traces. Perception 25, 543-67

Francis, G, Grossberg, S, and Mingolla, E. (1994). Cortical dynamics of feature binding and reset: control of visual persistence. Vision Research, 34, 1089-1104.

Freeman, A. W. (2005). Multistage model for binocular rivalry. Journal of Neurophysiology, 94, 4412-4420.

Gove, A., Grossberg, S., and Mingolla, E. (1995). Brightness perception, illusory contours, and corticogeniculate feedback. Visual Neuroscience, 12, 1027-1052.

Grossberg, S. (1968). Some physiological and biochemical consequences of psychological postulates. Proceedings of the National Academy of Sciences, U.S.A. 60, 758-765.

Grossberg, S. (1972). A neural theory of punishment and avoidance, II: Quantitative theory. Mathematical Biosciences, 15, 253-285.

Grossberg, S. (1976). Adaptive pattern classification and universal recoding, II: Feedback, expectation, olfaction, and illusions. Biological Cybernetics, 23, 187-202.

Grossberg, S. (1978). A theory of human memory: Self-organization and performance of sensory-motor codes, maps, and plans. In R. Rosen and F. Snell (Eds.), Progress in theoretical biology, Volume 5. New York: Academic Press, pp. 233-374.

Grossberg, S. (1980). How does a brain build a cognitive code? Psychological Review, 87, 1-51.

Grossberg, S. (1984). Outline of a theory of brightness, color, and form perception. In Trends in mathematical psychology, E. Degreef & J. van Buggenhaut eds. (North-Holland, Amsterdam), pp. 59-85.

Grossberg, S. (1987). Cortical dynamics of three-dimensional form, color, and brightness perception: II. Binocular theory. Perception and Psychophysics, 41, 117-158.

Grossberg, S. (1994). 3-D vision and figure-ground separation by visual cortex. Perception and Psychophysics , 1994, 55 , 48-120.

Grossberg, S. (1995). The attentive brain. American Scientist, 83, 438-449.

Grossberg, S. (1999). The link between brain learning, attention, and consciousness. Consciousness and Cognition, 8, 1-44.

Grossberg, S. (2003). How does the cerebral cortex work? Development, learning, attention, and 3-D vision by laminar circuits of visual cortex. Behavioral and Cognitive Neuroscience Reviews, 2, 47-76.

Grossberg, S., and Howe, P.D.L. (2003). A laminar cortical model of stereopsis and three-dimensional surface perception. Vision Research, 43, 801-829.

Grossberg, S., and McLoughlin, N. (1997). Cortical dynamics of 3-D surface perception: Binocular and half-occluded scenic images. Neural Networks, 10 , 1583-1605.

Grossberg, S, and Mingolla, E. (1985). Neural dynamics of perceptual grouping: Textures, boundaries, and emergent segmentations. Perception and Psychophysics, 38, 141-171.

Grossberg, S., and Raizada, R. (2000). Contrast-sensitive perceptual grouping and object-based attention in the laminar circuits of primary visual cortex. Vision Research, 40, 1413-1432.

Grossberg, S, and Seidman, D. (2006). Neural dynamics of autistic behaviors: Cognitive, emotional, and timing substrates. Psychological Review, 113, 483-527.

Grossberg, S, and Seitz, A. (2003). Laminar development of receptive fields, maps, and columns in visual cortex: The coordinating role of the subplate. Cerebral Cortex, 13, 852-863.

Grossberg, S, and Swaminathan, G. (2004). A laminar cortical model for 3-D perception of slanted and curved surfaces and of 2D images: development, attention, and bistability. Vision Research, 44, 1147-1187.

Grossberg, S, and Yazdanbakhsh, A. (2005). Laminar cortical dynamics of 3-D surface perception: stratification, transparency, and neon color spreading. Vision Research, 45, 1725-1743.

Grunewald, A., and Grossberg, S. (1998). Self-organization of binocular disparity tuning by reciprocal corticogeniculate interactions. Journal of Cognitive Neuroscience, 10, 199–215.

Hirsch, J.A., and Gilbert, C.D. (1991). Synaptic physiology of horizontal connections in the cat's visual cortex. Journal of Neuroscience, 11, 1800-1809.

Hubel, D.H. and Livingstone, M.S. (1987). Segregation of form, color, and stereopsis in primate area 18. The Journal of Neuroscience, 7, 3378-3415.

Kapadia, M.K., Ito, M., Gilbert, C.D., and Westheimer, G. (1995). Improvement in visual sensitivity by changes in local context: parallel studies in human observers and in V1 of alert monkeys. Neuron, 15, 843–856.

Kaufman, L. (1963). On the spread of suppression and binocular rivalry. Vision Research, 3, 401-415.

Kelly, F.J. and Grossberg, S. (2000). Neural dynamics of 3-D surface perception: Figure-ground separation and lightness perception. Perception & Psychophysics, 62, 1596-1619.

Kellman, P. J., and Shipley, T. F. (1991). A theory of visual interpolation in object perception. Cognitive Psychology, 23, 141-221.

Kovács, I., Papthomas, T.V., Yang, M., and Fehér, Á. (1996). When the brain changes its mind: interocular grouping during binocular rivalry. Proceedings of the National Academy of Sciences USA, 93, 15508-15511.

Laing, C.R., and Chow C.C. (2002). A spiking neuron model for binocular rivalry. Journal of Computational Neuroscience, 12, 39-53.

Lankheet, M. J. (2006). Unraveling adaptation and mutual inhibition in perceptual rivalry. Journal of Vision, 6, 304-310.

Lee, S.H., and Blake, R. (1999). Rival ideas about binocular rivalry. Vision Research, 39, 1447-1454

Lee, S.H., and Blake, R. (2002). V1 activity is reduced during binocular rivalry. Journal of Vision, 2, 618-626.

Leopold, D.A., and Logothetis, N.K. (1996). Activity changes in early visual cortex reflect monkeys' percepts during binocular rivalry. Nature, 379, 549-553.

Levelt, W.J. (1967). Note on the distribution of dominance times in binocular rivalry. British Journal of Psychology, 58, 143-145.

Liu, L., Tyler C.W., and Schor, C.M. (1992). Failure of rivalry at low contrast: Evidence of a suprathreshold binocular summation process. Vision Research, 32, 1471-1479.

Logothetis, N.K. (1998). Single units and conscious vision. Philosophical Transactions of the Royal Society of London, B, Biol. Sci. 353, 1801-1818.

Logothetis, N.K., Leopold, D.A., and Sheinberg, D.L. (1996). What is rivaling during binocular rivalry? Nature, 380, 621-624.

Logothetis, N.K., and Schall, J.D. (1989). Neuronal correlates of subjective visual perception. Science, 245, 761-763.

Lumer, E.D. (1998). A neural model of binocular integration and rivalry based on the coordination of action-potential timing in primary visual cortex. Cerebral Cortex, 8, 553-561.

Maier, A., Logothetis, N.K., and Leopold, D.A. (2005). Global competition dictates local suppression in pattern rivalry. Journal of Vision, 5, 668-677.

Matsuoka, K. (1984). The dynamic model of binocular rivalry. Biological Cybernetics, 49, 201-208.

McGuire, B.A., Gilbert, C.D., Rivlin, P.K., and Wiesel, T.N. (1991). Targets of horizontal connections in macaque primary visual cortex. Journal of Comparative Neurology, 305, 370-392.

Meyer, G., and Ming, C. (1988). The visible persistence of illusory contours. Canadian Journal of Psychology, 42, 479-488.

Meyer, G., Lawson, R., and Cohen, W. (1975). The effects of orientation-specific adaptation on the duration of short-term visual storage. Vision Research, 15, 569-572.

Mingolla, E., Ross, W., and Grossberg, S. (1999). A neural network for enhancing boundaries and surfaces in synthetic aperture radar images. Neural Networks, 12, 499-511.

Mitchell, J. F., Stoner, G. R., and Reynolds, J.H. (2004). Object-based attention determines dominance in binocular rivalry. Nature, 429, 410-413.

Mueller, T.J. (1990). A physiological model of binocular rivalry. Visual Neuroscience, 4, 63-73.

Mueller, T.J., and Blake, R. (1989). A fresh look at the temporal dynamics of binocular rivalry. Biological Cybernetics, 61, 223-232.

Ngo, T.T., Miller, S.M., Liu, G.B., and Pettigrew, J.D. (2000). Binocular rivalry and perceptual coherence. Current Biology, 10, 134-136.

Ögmen, H, and Gagné, S. (1990). Neural network architecture for motion perception and elementary motion detection in the fly visual system. Neural Networks, 3, 487-506.

O'Shea, R.P. (1998). Effects of orientation and spatial frequency on monocular and binocular rivalry. In Kasabov, N., Kozma, R., Ko, K. O'Shea, R., Coghill, G., and Gedeon, T. (Eds.). Progress in connectionist-based information systems: Proceedings of the 1997 International Conference on Neural Information Processing and Intelligent Information Systems, pp. 67-70. Singapore: Springer-Verlag.

Peterhans, E. (1997). Functional organization of area V2 in the awake monkey. Cerebral Cortex, 12, 335-357.

Peterhans, E., and von der Heydt, R. (1989). Mechanisms of contour perception in monkey visual cortex. II. Contours bridging gaps. The Journal of Neuroscience, 9, 1749-1763.

Poggio, G.F. and Fischer, B. (1977). Binocular interaction and depth sensitivity in striate and prestriate cortex of behaving rhesus monkey. Journal of Neurophysiology, 40, 1392-1405.

Pollen, D. A. (1999). On the neural correlates of visual perception. Cerebral Cortex, 9, 4–19.

Polonsky, A., Blake, R., Braun, J., and Heeger, D.J. (2000). Neuronal activity in human primary visual cortex correlates with perception during binocular rivalry. Nature Neuroscience, 3, 1153-1159.

Roe, A.W. and Ts'o, D.Y. (1997). The functional architecture of area V2 in the macaque monkey. Cerebral Cortex, 12, 295-333.

Roelfsema, P.R., Lamme, V.A.F., and Spekreijse, H. (1998). Object-based attention in the primary visual cortex of the macaque monkey. Nature, 395, 376-381.

Sheinberg, D.L., and Logothetis, N.K. (1997). The role of temporal cortical areas in perceptual organization. Proceedings of the National Academy of Sciences U.S.A. 94, 3408-3413.

Sindermann, R., and Lueddeke H. (1972). Monocular analogues to binocular contour rivalry. Vision Research, 12, 763-772.

Stollenwerk, L., and Bode M. (2003). Lateral neural model of binocular rivalry. Neural Compution, 15, 2863-2882.

Sur, M., Schummers, J., and Dragoi, V. (2002). Cortical plasticity: time for a change. Current Biology, 12, 168-170.

Thorell, L.G., DeValois, L.G., and Albrecht, D.B. (1984). Spatial mapping of monkey V1 cells with pure color and luminance stimuli. Vision Research, 24, 751-769.

Tucker, T.R., and Katz, L.C. (2003). Spatiotemporal patterns of excitation and inhibition evoked by the horizontal network in layer 2/3 of ferret visual cortex. Journal of Neurophysiology, 89, 488-500.

Van Tuijl, HFJM. (1975). A new visual illusion: Neonlike color spreading and complementary color induction between subjective contours. Acta Psychologica, 39, 441-445.

von der Heydt, R., Peterhans, E., and Baumgartner, G. (1984). Illusory contours and cortical neuron responses. Science, 224, 1260–1262.

Von der Heydt, R., Zhou, H., and Friedman, H.S. (2000). Representation of stereoscopic edges in monkey visual cortex, Vision Research, 40, 1955-1967.

Wade, N.J. (1973). Contour synchrony in binocular rivalry, Perception and Psychophysics, 13, 423-425.

Wade, N.J. (1975). Monocular and binocular rivalry between contours. Perception, 4, 85-95.

Wales, R., and Fox, R. (1970). Incremental detection thresholds during binocular rivalry suppression. Perception & Psychophysics, 8, 90-94.

Wheatstone, C. (1838/1952). Contributions to the physiology of vision. —Part the First. On some remarkable, and hithero unobserved, phaenomena of binocular vision. Philosophysical Magazine J. Sci., Series 4, 3, 241-267.

Wilson, H. R. (2003). Computational evidence for a rivalry hierarchy in vision. Proceedings of the National Academy of Sciences USA, 100, 14499-14503.

Wilson, H. R. (2005). Rivalry and perceptual oscillations: A dynamical synthesis. In Binocular rivalry, D. Alais & R. Blake, Eds. (MIT Press, Cambridge, London), pp. 317-335.

Wilson, H.R., Krupa, B., and Wilkinson, F. (2000). Dynamics of perceptual oscillations in form vision. Nature Neuroscience, 3, 170-176.

Yazdanbakhsh, A., and Watanabe, T. (2004). Asymmetry between horizontal and vertical illusory lines in determining the depth of their embedded surface. Vision Research, 44, 2621-2627.